IMPACT ASSESSMENT OF WATER JETS FROM FLIP BUCKETS

A THESIS SUBMITTED TO
THE GRADUATE SCHOOL OF NATURAL AND APPLIED SCIENCES
OF
MIDDLE EAST TECHNICAL UNIVERSITY

BY

CUNEYT YAVUZ

IN PARTIAL FULLFILLMENT OF THE REQUIREMENTS
FOR
THE DEGREE OF MASTER OF SCIENCE
IN
CIVIL ENGINEERING

AUGUST 2014

Approval of the thesis:

IMPACT ASSESSMENT OF WATER JETS FROM FLIP BUCKETS

Submitted by **CUNEYT YAVUZ** in partial fulfillment of the requirements for the degree of **Master of Science in Civil Engineering Department, Middle East Technical University** by,

Prof. Dr. Canan Özgen
Dean, **Graduate School of Natural and Applied Sciences** _____

Prof. Dr. Ahmet Cevdet Yalçıner
Head of Department, **Civil Engineering** _____

Prof. Dr. Ismail Aydın
Supervisor, **Civil Engineering Dept., METU** _____

Examining Committee Members:

Prof. Dr. Zafer Bozkuş
Civil Engineering Dept., METU _____

Prof. Dr. Ismail Aydın
Civil Engineering Dept., METU _____

Prof. Dr. A. Burcu Altan Sakarya
Civil Engineering Dept., METU _____

Assoc. Prof. Dr. Mete Köken
Civil Engineering Dept., METU _____

M.S. in CE Edip Öztürel
ENSU A.Ş. _____

Date: _____

I hereby declare that all information in this document has been obtained and presented in accordance with academic rules and ethical conduct. I also declare that, as required by these rules and conduct, I have fully cited and referenced all material and results that are not original to this work.

Name, Last name: Cuneyt YAVUZ

Signature:

ABSTRACT

IMPACT ASSESSMENT OF WATER JETS FROM FLIP BUCKETS

Yavuz, Cüneyt

M.S., Department of Civil Engineering

Supervisor: Prof. Dr. İsmail Aydın

August 2014, 63 Pages

A jet issued from flip bucket of spillway of a dam interacts with the surrounding air and develops into an aerated turbulent jet. Depending on the relative jet thickness, the fall height and the level of turbulence, the jet may be dispersed in air forming an aerated water body which will eventually plunge into the river surface at sufficiently far downstream of the flip bucket. If not aerated, the jet may have a larger impact on the river bed causing severe scour damage. Water cushion and dispersion of jet by aeration are the practical tools to reduce the jet impact. An experimental study is conducted to analyze the contribution of water cushion to damp the dynamic pressures on the bed. The jet impact is analyzed using geometric elements of the jet trajectory in an effort to characterize the jet impact conditions in terms of relevant dimensionless parameters. It is observed that aeration of the jet is more effective in minimizing the impact when compared to the contribution of water cushion depth.

Keywords: Water Jet, Flip Bucket, Impact Assessment, Water Cushion, Jet Dispersion, Air Entrainment, Scour

ÖZ

SIÇRATMA EŞİĞİNDEN GELEN SU JETİ DARBE ETKİSİNİN DEĞERLENDİRİLMESİ

Yavuz, Cüneyt
Yüksek Lisans, İnşaat Mühendisliği Bölümü
Tez Yöneticisi: Prof. Dr. İsmail Aydın

Ağustos 2014, 63 Sayfa

Dolusavak üzerindeki sıçratma eşiğinden çıkan bir jet, kendini çevreleyen hava ile etkileşime girerek hava karışımlı türbülanslı bir jet oluşturur. Jet kalınlığı, düşü yüksekliği ve türbülans derecesine bağlı olarak, havada dağılan jet sonunda sıçratma eşiğinin mansabındaki yeterince uzak bir noktada nehrin yüzeyine çarpar. Eğer yeterince havalanmazsa, jet mansap tarafındaki nehir yatağında önemli oyulmalara neden olan büyük bir darbe etkisi yaratabilir. Su yastığı ve jetin hava içinde yayılması, darbe etkisini azaltmak için pratik yöntemlerdir. Su yastığının nehir yatağındaki dinamik basınçları düşürmedeki etkisini görmek için deneysel bir çalışma yürütülmüştür. Jet darbe etkisini ilgili boyutsuz parametrelerle karakterize edebilmek amacıyla geometrik değişkenler kullanılarak jet darbe etkisi analiz edilmiştir. Darbe etkisini azaltma açısından jetin havalanmasının su yastığı derinliğinden daha etkin bir yöntem olduğu gözlenmiştir.

Anahtar kelimler: Su jeti, Sıçratma Eşiği, Havalanmış Jet, Darbe Etkisi, Su Yastığı, Jet Yayılması, Hava Girişi, Oyulma

To my precious family

ACKNOWLEDGEMENTS

First of all, I wish to express my deepest gratitude to my supervisor Prof. Dr. Ismail Aydin, for his valuable guidance, patience, encouragement and support throughout the conduction of experiments and preparation of this thesis.

I would like to express my sincere gratitude to Prof. Dr. Mustafa Aral, for his support, encouragement and confidence in me to complete this thesis.

Most importantly, my special thanks to go to a wonderful friend, Ali Ersin Dinçer. Without his constant support and guidance, the completion of this thesis would not be possible.

I am also grateful to my friend Kutay Yilmaz for his help during different phases of my study and my thesis.

Additional gratitude goes to Mükremin Daştan for his continuous and unique encouragement and moral support in many ways.

I appreciate my friends Siamak Gharahjeh, Ahmet Nazım Şahin, Emre Haspolat, Ezgi Köker, Nilay İşcen and Tuğçe Yıldırım who are my colleagues and friends in the Hydromechanics Division.

Finally, words cannot express my appreciation for my lovely wife Derya Yavuz and my beloved daughter Zeynep Yavuz whose lifelong love, support and encouragement have kept me doing.

To all these, and to the many other friends and family who have helped me, I can only express my gratitude and sincere.

TABLE OF CONTENTS

LIST OF TABLES

TABLES

LIST OF FIGURES

FIGURES

LIST OF SYMBOLS

A_w	:	Water area at impingement point (m^2)
A_a	:	Air area at impingement point (m^2)
a	:	Width of the dispersed jet at impingement point (m)
b	:	Length of the dispersed jet at impingement point (m)
C_d	:	Discharge coefficient for rectangular channel
d	:	Tail water depth
d^+	:	Normalized tail water depth
$(Fr)_m$	:	Model Froude number
$(F_r)_p$	:	Prototype Froude number
g	:	Gravitational acceleration (m^2/s)
h_j	:	Water depth on the bucket lip (m)
h_L	:	Head loss due to the air entrainment (m)
H_{res}	:	Water level in the reservoir (m)
H_T	:	Total head at the bucket lip (m)
H_{j1}	:	Jet head without considering air entrainment (m)
H_{j2}	:	Hypothetical Jet head without considering air entrainment (m)
L_m	:	Model scale
L_p	:	Prototype scale
L_r	:	Length ratio
V_m	:	Model velocity (m/s)
V_p	:	Prototype velocity (m/s)
L_t	:	Trajectory length without considering air entrainment (m)
$(L_1)_m$	:	Measured Trajectory length considering air resistance (m)
$(L_1)_c$	:	Calculated Trajectory length considering air resistance (m)
k	:	Constant related to air resistance
Q	:	Water discharge (m^3/s)
P	:	Height of the sharp crested weir (m)
P^+	:	Normalized dynamic pressure head
P_d/γ	:	Dynamic pressure head (m)
P_T/γ	:	Total pressure head (m)
P_h/γ	:	Hydrostatic pressure head (m)
V_j	:	Velocity at the bucket lip (m/s)
V_t	:	Velocity at impingement point (m/s)
w	:	Channel width (m)
z_i	:	Vertical drop from lip to tail-water level (m)
α	:	Trajectory length constant from Equation 6

α_j	:	Flip bucket lip angle (degree)
α_t	:	Trajectory angle (degree)
γ	:	Specific weight of water (N/m^3)
Re	:	Reynolds Number
We	:	Weber Number
Fr	:	Froude Number

CHAPTER 1

INTRODUCTION

1.1 Introduction

One of the significant issues nowadays is water management due to the lack of water for energy production and water supply. Because of this reason, dams were built to kept large amount of water behind them. This quantity of water creates a potential threat for downstream reaches and safety of the dam itself. The safe design of a dam includes a spillway which is used for the release of water from the dam.

''He who creates a potential danger is responsible for doing everything within human power to manage it.'' (Anonym)

It is important to understand the legal argument above to clarify the function of the spillway.

Although spillways can be used for releasing the excess water coming from the dam, it is not enough for dissipating the energy of the water. Because this amount of water could have an enormous energy and this energy can be a reason for problems at the downstream of the dam such as scour. Therefore, suitable energy dissipating system has to be installed on the downstream sections of the spillway. These systems may consist of several applications.

Dissipating the kinetic energy of the water jet coming from the spillway is essential before the impingement point of the jet into the downstream river reach to prevent the riverbed from scour banks from erosion. Dissipating the energy of the water jet is also necessary for the protection of dam and adjacent structures like powerhouse, canal as well as the spillway.

In order to dissipate the energy of the water coming from the spillway, some energy dissipation structures can be used such as ski jump, plunge pool, baffle blocks, hydraulic jump etc. may also create some problems like scour, cavitation at the plunge pool floor and bank erosion. These problems need to be identified and solved.

1.2 Spillways

1.2.1 Necessity of a Spillway

Spillways are designed to prevent overtopping of a dam when there is excess water in the reservoir. The importance of a spillway was discussed by Vischer et al. (1988) with the following questions:

Is overtopping of the excess water possible from the reservoir?

Could overflowing cause a dam brake?

Could overtopping the excess water cause another damages?

If the capacity of the reservoir is lesser than difference between the volumes of inflow and outflow, this reservoir will overflow. If a dam can be built high enough to hold the whole volume of inflow, no spillway would be essential and an outlet such as a turbine or sluice gate would solely be needed for regulating and using the water in the reservoir. But generally, it is not applicable. Therefore, spillway is necessary to discharge the extra quantity of water from the reservoir.

The necessity of the spillway is obvious for the safety of the dam against overtopping. Due to this necessity, the cost of the spillway should be taken into consideration for the economical point of view.

If the cost of a spillway is compared with the total cost of a dam, percentage of the total cost of spillway shows a large variation. It is setting up from 4% (unlined rock spillways) to 22% (spillways for earth and rock-fill dams) (Khatsuria, 2005). Dam safety is another issue should also be considered for the aims of spillway construction. One of the United States Bureau of Reclamation (USBR) report (1983) proclaims that 40% of the dam failure hazards occur due to the spillway insufficiency. If the benefits of the spillway are assess like this, the percentage cost of the spillway is commonly much lower.

1.2.2 Functions of Spillway

Takasu et al. (1988) discussed and concluded especially seven functions that can be assigned to spillway.

i. Maintaining normal river water functions
ii. Discharging water for utilization
iii. Maintaining initial water level in the flood-control operation
iv. Controlling floods
v. Controlling additional floods
vi. Releasing surplus water
vii. Lowering water levels

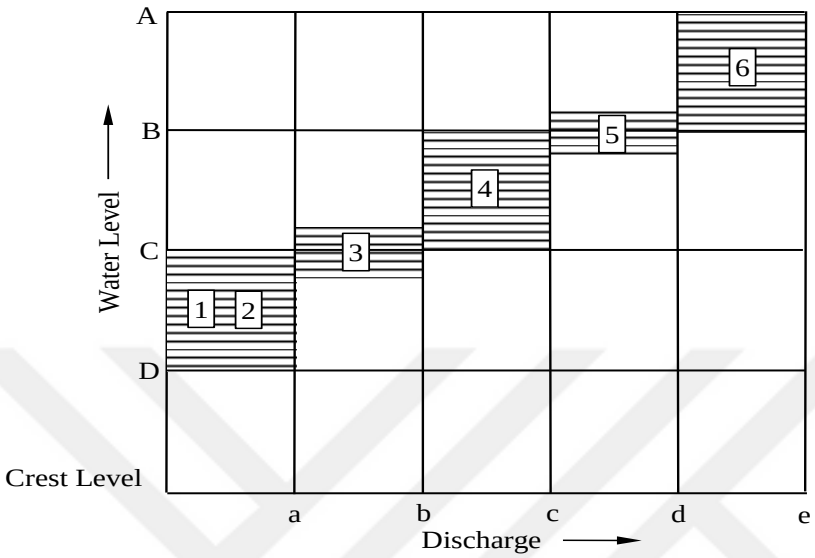

Figure 1 Function of Spillways and Regulating Outlets. (Takasu et al.-1988)

A: Design flood level, B: Surcharge level, C: Initial water level in flood-control operation, D: Minimum operating level, a: Maximum outflow for water supply, b: Initial inflow discharge in the flood-control operation, c: Maximum outflow discharge in the flood-control operation, d: Standard project flood discharge, e: Spillway design flood discharge, 1: Maintenance of normal river water functions (compensation water), 2: Discharge for water utilization, 3: Maintaining initial water level in flood-control operation, 4: Flood control, 5: Additional flood control, 6: Release of surplus water.

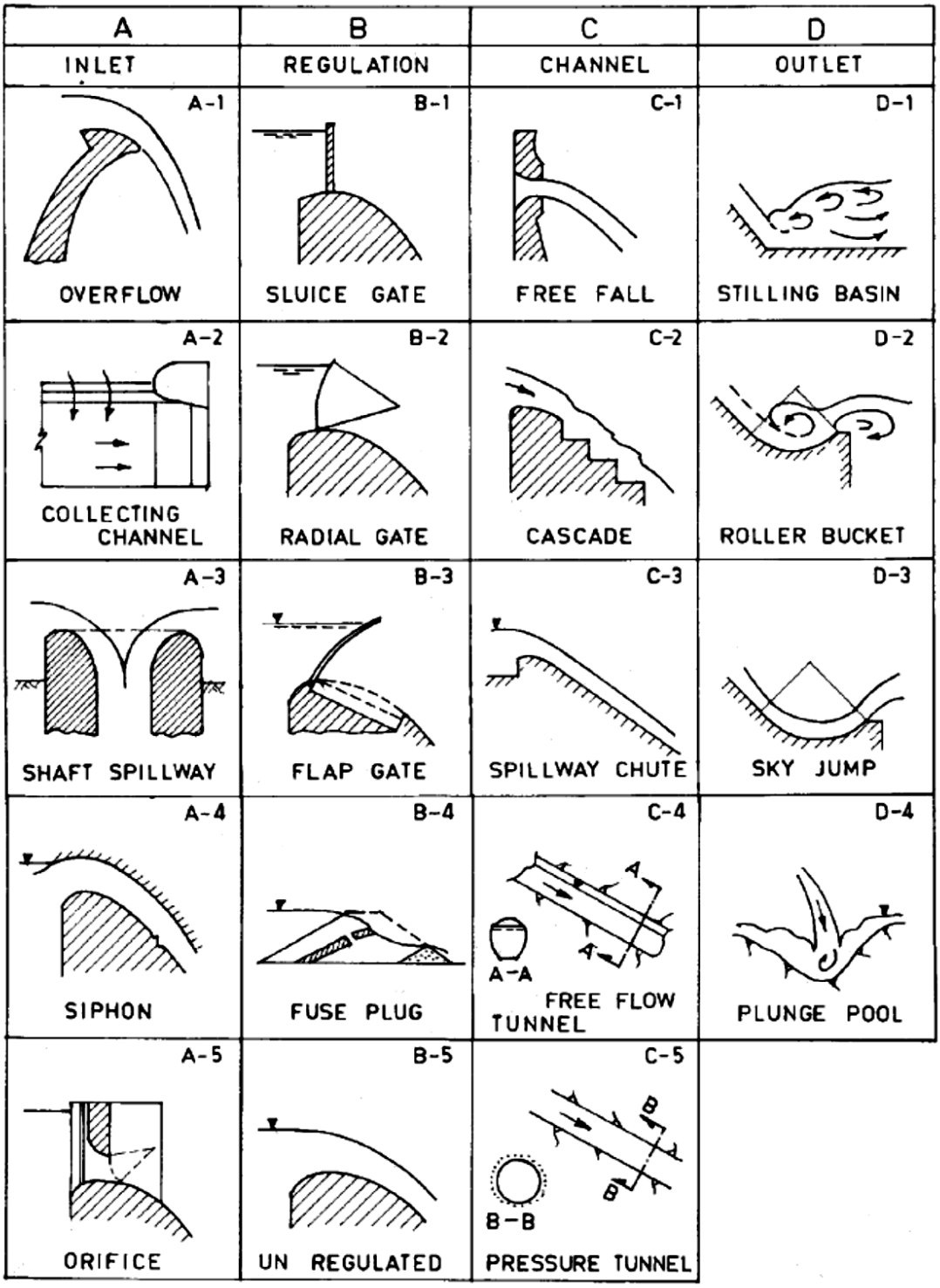

Figure 2 Classification of Spillway (shown in Vischer et al, San Francisco, 1988).

1.2.3 Classification of Spillways

Spillways have been classified by Khatsuria (2005) according to various criteria

I. Feature of the spillway

a) Stepped spillway
b) Labyrinth spillway
c) Siphon spillway
d) Side channel spillway
e) Shaft spillway
f) Straight drop or overfall spillway
g) Tunnel spillway or Culvert spillway
h) Chute spillway
i) Ogee spillway

II. Function of the spillway

a) Auxiliary spillway
b) Service spillway
c) Fuse plug or emergency spillway

III. As a Control Structure

a) Orifice of sluice spillway
b) Ungated spillway
c) Gated spillway

More detailed classification was proclaimed by Vischer et al. (1988) basically all components of the spillway. Following options in each component is shown in Figure 2.

1.3 Energy Dissipators for Spillways

1.3.1 Classification of Energy Dissipators

Classification of energy dissipators for the spillways can be define under the following four categories (Khatsuria, 2005):

i. Geometry or form of the structure
ii. Geometry or form of the main flow
iii. Hydraulic action
iv. Dissipation mode

Structural form of the energy dissipators such as bucket, stilling basin apron, etc. is the most reliable classification method.

1.3.2 Principal Types of Energy Dissipators

The energy dissipators can be classified according to structural point of view such as (Khatsuria, 2005):

i. Free jets and trajectory buckets
ii. Roller buckets
iii. Hydraulic jump stilling basins
iv. Dissipation by spatial hydraulic jump
v. Impact type energy dissipators

Actually, free jets and trajectory buckets deflect the high velocity jet into the air and significant amount of energy dissipates due to air entrainment. Additionally, jet hits the river bed at a large distance from the structure. If any scour that may happen in the impingement area, it stays away from the structure and does not threaten the stability of the structure.

Roller buckets are used to create a hydraulic jump on a curved floor. Hydraulic jump occurred on the roller bucket is connected to the Froude number of the flow coming from the spillway and tail-water depth.

Hydraulic jump stilling basins contain basins prepared with energy dissipating components such as chute blocks, baffle piers, horizontal and sloping aprons and saw-like end sills. This type of energy dissipators are commonly used for the spillways. Its performance is also closely connected to the Froude number of the incoming flow and affects up to 60% dissipation of the energy incoming the basin.

Another type of the energy dissipator is a flip bucket. If the construction area is limited, this type of energy dissipators are convenient to apply. Like free jets, flip buckets deflect the water jet into the air. Because of the air resistance, energy of the jet dissipates and this jet hits the river bed at a large distance from the dam.

Impact type energy dissipators are used to reduce the energy of the water by creating the hydraulic jump. This method can be practical to achieve energy dissipation in small chutes and spillways.

Nowadays, stepped spillways are also used as an energy dissipator. Because it matches the characteristics of both the spillway and energy dissipators. These are appropriate for dams being constructed with roller compacted concrete (RCC). However, their use is limited up to the unit discharge of 30 $m^3/s/m$ due to the cavitation damage probability.

1.3.3 Selection of the Type of Energy Dissipator

Some factors play an important role on selection of the type of energy dissipator. They are: type of the dam, layout of other connected structures, hydraulic concerns, landscape, geology, inflow and outflow amounts, dam height, economic assessment etc.
According to the above criterias manuals change for the types of energy dissipators can be employed. Mason (1982) has mentioned, ‘‘that the design of prototype hydraulic energy dissipators is not the exact science that design charts sometimes suggest is

confirmed by the problems that continue to be reported with all types of dissipator.'' In order to define the variety of the applications of energy dissipators Mason conducted a literature survey of 370 prototype dissipators from dams in 61 countries. He gathered these energy dissipators in six groups: hydraulic jump basins, free jets, rock basins, baffle basins, ski jumps, and flip buckets. He used total head, H and total discharge, Q as hydraulic parameters of this classification.

1.4 Trajectory Buckets

1.4.1 Types and Classification of Trajectory Buckets

Trajectory buckets can be named as; free jet spillways, free over-falls, trajectory bucket, ski jump bucket and flip bucket. Mason (1982) describes ski jumps as jets issuing at the downstream of a dam and flip buckets placed at the end of spillway away from the main body of the dam.

Trajectory bucket represents free jet spillways, ski jump buckets, and flip buckets. The ski jump buckets are installed above the river bed, with or without the power house underneath the bucket as shown in Figure 3. Flip buckets are built at the foot of the spillway or at the outlet of a tunnel as shown in Figure 4.

Free jet spillways are applicable for the high velocity jet issues from either a short crested spillway at the top of an arch dam or a deep settled short length bottom outlet as shown in Figure 5.

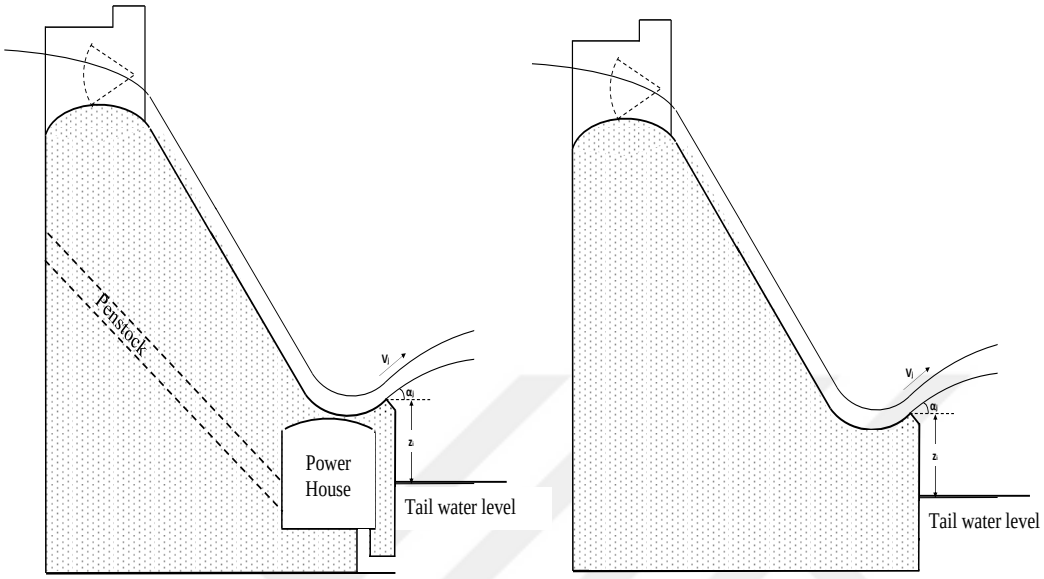

Figure 3 Ski jump buckets

In a free jet spillway, the jet is exposed to air resistance and air entrainment. Due to air entrainment, important amount of energy dissipates before the jet plunges into the tail-water. Further dissipation of energy occurs due to water cushion in the river bed. Actually, the main goal of the ski jump bucket is to have jet impinge at as great a distance downstream as possible so that the main dam is not threatened by the scour.

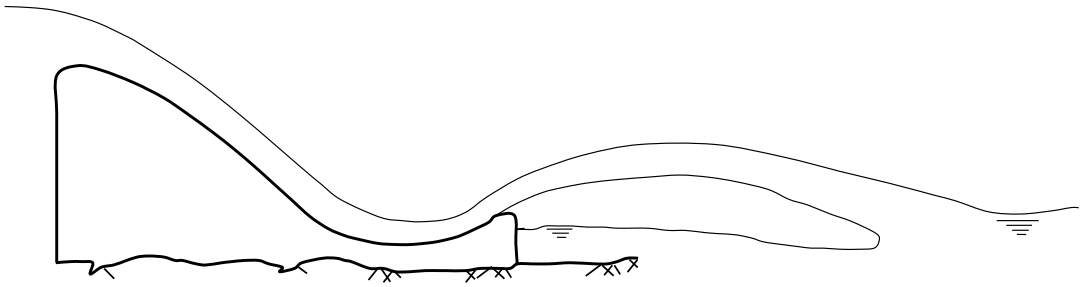

Flip Bucket on Overflow Spillway

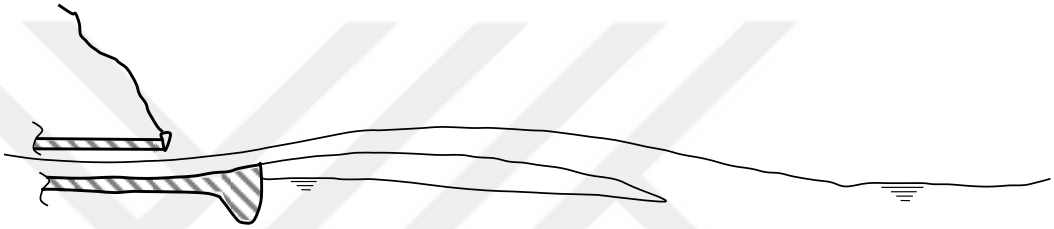

Flip Bucket on Tunnel Spillway

Figure 4 Flip buckets

In a flip bucket, dissipation of energy is generally created by water cushion and air entrainment. Determination of the total energy dissipation ratio created by these reasons are another concern for the engineers.

1.4.2 Design of Bucket Components

The components of the flip bucket can be classified as following:

i. Shape of the bucket
ii. Invert elevation
iii. Bucket radius
iv. Lip angle

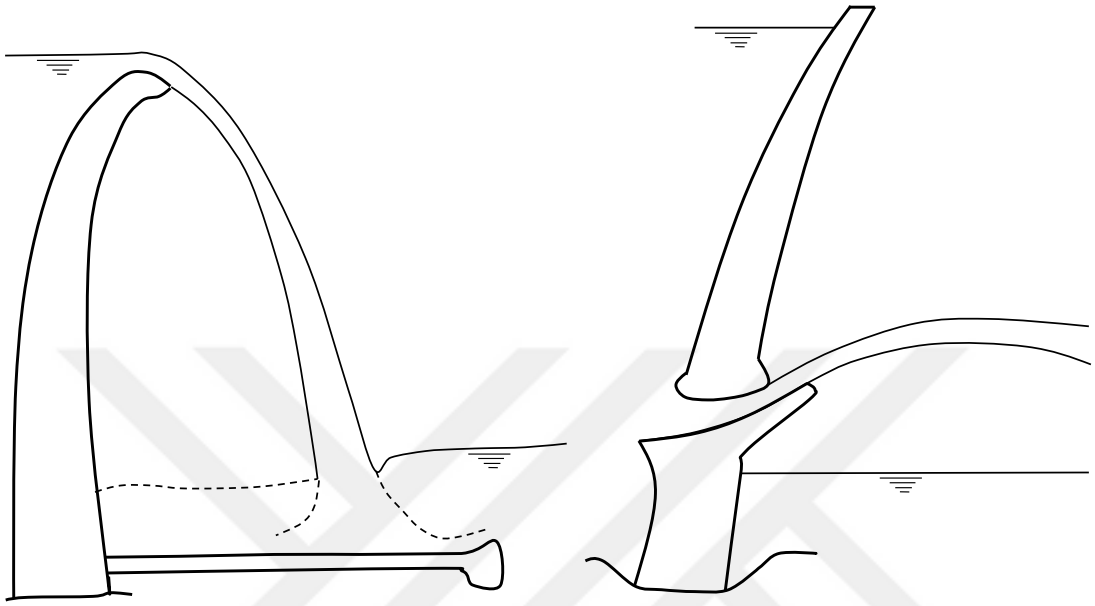

Figure 5 Free jet spillways

Mason (1993) mentions ‘‘few designers would have confidence in a bucket invert for high velocity flow formed by anything other than smooth curves’’ shows an inclination in favor for a circular arc for the shape of the flip bucket.

Invert elevation of the buckets mostly depend on topographic conditions. If a rock layer exists at the construction site, this layer may be used in order not to use large quantity of concrete. Bucket lip elevation also depends on invert elevation, bucket radius, and lip angle. Tail water depth is another criteria for the determination of the lip elevation.

Bucket radius can be affected from the total head, the discharge amount, and the depth of overflow.

Bucket lip angle is imposed by the necessity of the trajectory length and trajectory angle at impingement point. According to projectile motion theory, the longest throw is obtained when the jet leaves the bucket at an angle of 45 degree. If the tail water level is at the same

level as that of the lip elevation, the trajectory angle is the same as lip angle without considering head loss. But, generally trajectory angle is larger than bucket lip angle due to the elevation difference of the tail water depth and lip elevation.

1.5 Scour Downstream of Trajectory Buckets

Significant amount of scour can be formed at the downstream of the trajectory buckets due to the impinging water jet coming from the reservoir. Mason (1984) experienced that undesirable scour is not only limited to soft rocks but also some other cases may exist on igneous rocks. Several hundred tons rocks have been shifted by the flow. One of the bad circumstances of scour is moving towards the structure. Stability of the structure is threatened because of this type of scour and special precautions should be applied to avoid this danger.

1.5.1 Computation and Prediction

Depth of scour can be predicted using four common methods listed below (Khatsuria 2005):

i. Numerical analyses with laboratory studies.
ii. Numerical analyses with prototype observations.
iii. Experimental relations based on prototype observations.
iv. Laboratory tests for specific project

1.5.2 Analysis of the Possible Effects of Scour

Possible effects of scour can be defined by using experimental results and prototype observations. Some predictions and analysis applied for the effects of scour are:

i. Scour depth, location of scour and shape should be clearly predicted by comparing the model and prototype values.

ii. Estimation of scour amount approaches towards the dam body.
iii. Construction of bucket lip, retaining wall, etc. by considering the scour depths.

The depth and location of the scour should coincide with prototype and model. The experimental results obtained from the model and observations in the prototype may ultimately approach each other with an erodible bed.

1.5.3 Scour control and dispositions

Total prevention of the scour on the river bed is impossible on the riverbed. However, by constructing a plunge pool depth and location of the scour can be controlled. Some additional measurements can also applied in the downstream of the flip bucket.

Determination of solution at impact area on the riverbed requires experimental studies on the model and numerical calculations by using these data. If the impact assessment of the jet can be identified correctly on the riverbed by using model, the scour control mechanisms can be easily applied to the prototype.

1.6 Literature Survey

Ski jumps were particularly studied in France between 1930s and 1950s (Godon 1936; Coyne 1944, 1951; Auroy 1951). Investigations on the ski jumps were introduced with prototype observations performed on the water jets by Maitre and Obolensky (1954). Rajon and ShivashankaraRao (1980) summoned up the investigations about ski jump flow and prepared a guideline to design a flip bucket on the prototypes as described below;

a) Shape of the bucket should be circular
b) Deflection angle of the flip between 20^0 and 40^0.
c) Bucket radius should be selected depending on the bucket velocity and specific discharge of the flow.
d) The take-off part of the bucket is designed against cavitation phenomena.

e) Bucket should be above the tail-water.

Mason (1993) collected the studies on ski jump and recommended some points of design as follows;

a) Minimum bucket radius should be designed three out of five times the approach flow depth of the bucket.
b) Take off angle of the flip bucket between 20^0 and 35^0.
c) Water jet should be spread in air with the angle of 5^0.
d) Lip of the bucket ought to be flat due to the cavitation risk.

When these considerations were made the scour was not taken into account. Khatsuria (2005) decided to investigate the general form of the ski jump to identify the whole purpose of it. They noticed that most of the investigation of the sky jump design was made only for specific projects not in general form. So they mentioned that there has not been prepared a complete ski jump design guideline yet.

Heller et al. (2005) considered the 2-D ski jump. They worked on the scale effects of the water jets and found that aerated water jets required the approach flow depth of 40 mm at least. They also examined the pressure distribution on the components of ski jumps such as flip bucket and take-off angles of the jet trajectories. They employed point gauges to measure the jet trajectories. It was shown that the lower and upper jet trajectories have different take-off angle from the bucket angle with parabolic shape depending on the Froude number and relative approach flow depth.

Lukas Schmocker et al. (2008) focused on the analysis of the jet air entrainment characteristics of a plane jet downstream of a ski jump with and without aerated approach flow conditions. They changed the discharge which resulting the change of the flow depth on the spillway and variation of the Froude number. Via this experimental study they analyzed that the air concentration of the jet and its distribution, determination of the region of the minimum air concentration along the jet flow and evaluation of the air

entrainment characteristics of water jet on which the circular-shaped bucket placed at the take-off of ski jump. They used the hydraulic model of Heller et al (2006).

Weilin Xu et al. (2004) performed a series of experiments in a glass flume and a set of nozzle systems were used to produce plane jets. They investigated the effect of aeration on plane jet scour. Aerated and non-aerated jets were applied under the same conditions of tail-water depth, water discharge per unit width and jet velocity. Scour hole profile originated rely on primarily bed material and tail-water depth. Scour holes were compared and it was found that the scour holes formed similar to each other under aerated and non-aerated conditions.

Johnson (1967) conducted some experiments with a compact water jet, an air-water jet and a dispersed jet to study scour. Experimental set-up was consisting of a tank with a vertical jet nozzle and a gravel bed. He performed the tests and found that aeration of water jet reduces scouring the river bed nearly half of the tail-water depth required for no scour with the water jet.

Mason (1985, 1989) brought out many formulas about prediction of scour depth and found that scour might be affected by the percentage of air entrainment. He derived (Mason 1989) a new formula to calculate the scour depth by aerated jets through a set of experiments. Mason found that the scour profiles caused by aerated jets are flatter than those caused by non-aerated jets.

Bohrer et al. (1998) examined the plunge pool velocity decline of a free fall jet. He evaluated fully aerated jet and non-aerated jet and reasoned that aeration of jet decreases the jet velocity so the scour depth in water.

Mason and Aramugam (1995) studied on free jet scour at the downstream of the dams and flip buckets. They evaluated the accuracies of the formulas which were used for the estimation of the amount of scour below dam over falls and flip buckets. They worked on the data obtained from prototypes and models of the prototypes respectively. It is

demonstrated that these formulas are not precise enough for calculating ultimate scour depth of prototypes even though they are applicable for models. So, they introduced a new formula for estimating the scour depth which includes a permission for tail-water depth to give enhanced accuracy for models and prototypes.

E.F.R. Bollaert (2010) worked on scour formation of rock at the downstream of high-head hydraulic structures through turbulent air-water mixtures. Jet issuance from the dam, jet fall through the air and jet diffusion through the water cushion were studied. He performed a large series of experiments and clearly defined that use of small scale physical models may importantly change the predictions of scour depth. In order to obtain reliable scour predictions, flow turbulence, jet and aeration of plunge pool should be properly reproduced. After all these tests he concluded that when these parameters are available air can be estimated based on observations, numerical model can be used to predict scour formation and evaluation of the ultimate scour depth can be possible on the long term.

Rhone and Peterka (1959) studied on the flip buckets applied by the U.S Bureau of Reclamation.

Ample studies were conducted on the curvature of the bucket in order to identify pressure head and pressure distribution on the circular-shaped flip bucket by Balloffet (1961).

Henderson and Tierney (1963) found that for the ratio of flow depth, h_0, in the bucket is relatively small to its radius, R, of curvature by using a potential flow approach the deflection angle should be at least 45^0.

Lenau and Cassidy (1969) demonstrated that the effect of gravity is more significant than the effect of viscosity in bucket flow. The velocity head is much higher than the static head on the bucket. Hence, they showed that maximum pressure depends on the ratio of the flow depth to bucket curvature radius and Froude Number on the flip bucket.

Steiner R., Heller V., Hager W.H., and Minor H.E. (2008) decided to investigate the effects of the triangular-shaped flip bucket placed at the take-off of ski jump rather than the general form of the circular-shaped bucket. They obtained the following results which can be significant for the design of the flip bucket. Pressure on the flip bucket depends on the approach flow Froude number and the deflector angle of the bucket. They found the limits of the Froude number according to their model to prevent choking of the spillway bucket. They analyzed the shock wave heights which depend on Froude number and the oscillation zone below the trajectory jet in prismatic channel. Energy dissipation of the water jet depends on the deflector angle of the flip bucket and the drop height of the bucket take-off to the channel.

Ervine and Falvey (1987) and Ervine et al. (1997) showed that the presence of air bubbles inside the shear layer reduces the mean dynamic pressures on the plunge pool floor. They also considered, as a simplification that the flow velocity reduction in aerated conditions is negligible.

LIU Peiqing, GAO Jizhang, and LI Yongmei (1997) conducted an experimental investigation of the submerged impinging jets in a plunge pool downstream of large dams (Figure 6). The characteristics and energy dissipation mechanism of the submerged impinging jet in the plunge pool were investigated in details. Energy dissipation was examined related to turbulent shear and diffusion of the flow and viscous effects by the mean velocity gradient.

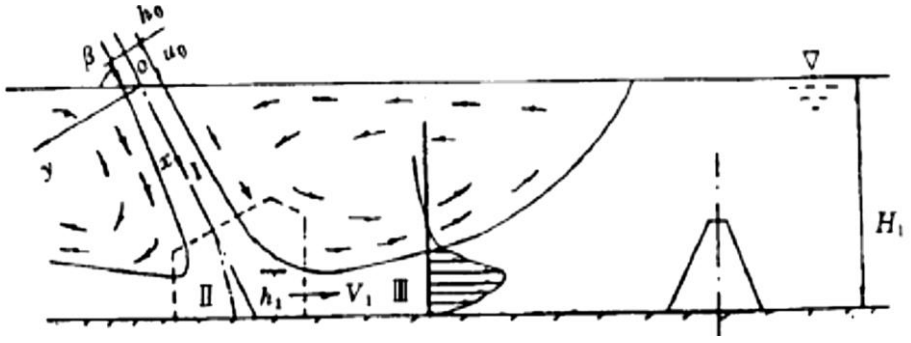

Figure 6 A submerged impinging jet in a plunge pool

Dong Z., Su P. (2003) dealt with a scour and dynamic pressure of impinging jet with and without aeration in the plunge pool. They performed over 30 empirical formulas related to the depth of scour. They mentioned that there are some differences between calculated results and measured data. The maximum error was 400 % and the minimum was 30 %. They conducted some experiments relevant with the impinging dynamic pressure on the plunge pool bottom, correlation and frequency-spectrum properties of pressure fluctuation, effects of air entrainment on time averaged pressure, pressure fluctuation including time averaged, and fluctuation distribution of pressure, etc. They stated that the high velocity jet issued from flip buckets have entrained a large amount of air in the process of diffusion and form high concentration air-water 2 phase flow. In addition the impinging jets entrain air at the point of entry as well. So they concentrated at the jet impinging point and collected the data at that point.

Ursino N., Salandin P., Deppo L. (2003) performed a laboratory set of experiments to investigate the pressure fluctuation field at the bottom of the plunge pool exposed to jet impingement. They stated that the knowledge of the stresses at the basis of plunge pool dissipation basins can be beneficial to predict a localized erosion process. They discussed the effect of a variable water cushion depth on the reduction of the drastic pressure fluctuations that occur on the beneath of a plunge pool with reference to the specific case of the prototype of a dam spillway and downstream energy dissipation basin. The experiments were conducted on a 1:40 laboratory model. Dynamic activity of pressure fluctuations were recorded in a set of various positions at the bottom of the plunge pool. They stated that the fluctuation pressure can be obtained increasing the cushion depth at the plunge pool. The experimental results were presented in dimensionless form.

Kawakami (1973) presented results of some field research on trajectories affected because of air resistance and defined a coefficient, k, as an aeration constant to determine the trajectory length with air resistance.

1.7 Scope of the Study

The aim of this study is to assess impact of the water jets from flip buckets at the impingement area on a riverbed. Hydraulic model of Laleli Dam and Hydroelectric Power Plant will be used as the test setup. Dynamic pressures on the bed will be measured for different water depths in the impingement area. Contribution of water in the river as water cushion to damp the pressure forces will be investigated.

In Chapter 2, method to calculate the jet trajectory length with relevant parameters is presented. Chapter 3 includes the description of experimental equipment, experimental procedure and results of the experiments. A comprehensive study is conducted on the experimental results, data is processed and comparisons of the calculated and measured experimental results are given in Chapter 4. Evaluation of the results and some dimensionless graphs related to determination of the flip bucket angle, trajectory angle, and head loss due to the air entrainment will also be given in Chapter 4. Conclusions of the study and recommendations are given in Chapter 5.

CHAPTER 2

CALCULATION OF FLOW AND JET CHARACTERISTICS

2.1 Discharge Calculation

Sharp-crested weir is a basic and suitable device for discharge measurements especially in rectangular open channels. A head-discharge relationship is generally developed to calculate discharge of flow over a sharp-crested weir and is shown in Eq. (1)

$$Q = \left(\frac{2}{3}\right) C_d w \sqrt{2gH^3} \quad (1)$$

where

C_d = Discharge coefficient
H = Water level above the weir crest
w = Channel width

Several studies had stated that the discharge coefficient is a function of flow conditions and weir geometry. Rehbock's experimental results (1929) are presented in Eq. (2)

$$C_d = 0.611 + 0.08\left(\frac{H}{P}\right) \qquad \text{for } \frac{H}{P} \leq 5 \quad (2)$$

where P = Height of the sharp crested weir.

2.2 Free Trajectory and Throw

The profile of the trajectory leaving a bucket depends on the velocity at the bucket lip, V_j and lip angle, α_j. The jet trajectory under the action of gravity can be computed (ignoring

friction and all kind of resistances) on the basis of projectile theory, resulting in the following expression (Khatsuria, 2005)

$$\frac{L_t}{H_j} = \sin 2\alpha_j + 2\cos\alpha_j \left(\sin^2\alpha_j + \frac{z_i}{H_j}\right)^{0.5} \quad (3)$$

where

L_t = Trajectory length without considering air entrainment,

z_i = Bucket lip height from tail water level,

H_j = Velocity head of the jet at bucket lip ($V_j^2/2g$),

α_j = Flip bucket lip angle, (degrees)

Eq. (3) can be rearranged and written as follows;

$$L_t = \frac{V_j \cos\alpha_j}{g}\left(V_j \sin\alpha_j + \sqrt{\left(V_j \sin\alpha_j\right)^2 + 2gz_i}\right) \quad (4)$$

Various parameters related to projectile motion of the jet are defined in Figure 7.

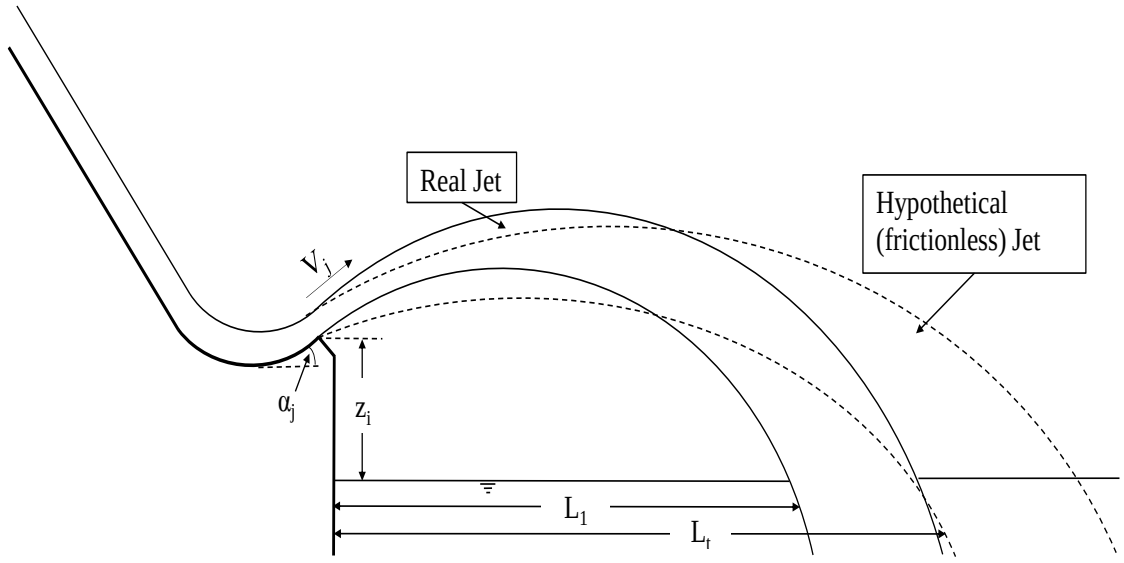

Figure 7 Throw distance of jet

The velocity head H_j at the bucket lip can be calculated by accounting the head losses from reservoir up to the bucket lip. Peterka (1978) has presented diagrams for throw distances for the flip buckets at the subgrade of tunnel spillways, where a horizontal length of tunnel portion is finished by the bucket. Air resistance, mainly for velocities above 20 m/s, affects the throw distance in the prototype. Kawakami (1973) presented results of some field research on trajectories affected because of air resistance and defined a coefficient, k for the following equations

$$L_1 = \left(\frac{1}{gk^2}\right) \ln\left(1 + 2k\alpha V_j \cos \alpha_j\right) \tag{5}$$

where

$$\alpha = \tan^{-1}\left(kV_j \sin \alpha_j\right) \tag{6}$$

and

L_1 = Throw distance considering air resistance

k = Constant related to air resistance

V_j = Velocity at the bucket lip

Figure 8 shows experimental relationship between V_j and k and also L_1/L_t values for different values of V_j, where L_t is the throw distance without considering the air resistance. α_t represents the trajectory angle at the impingement point.

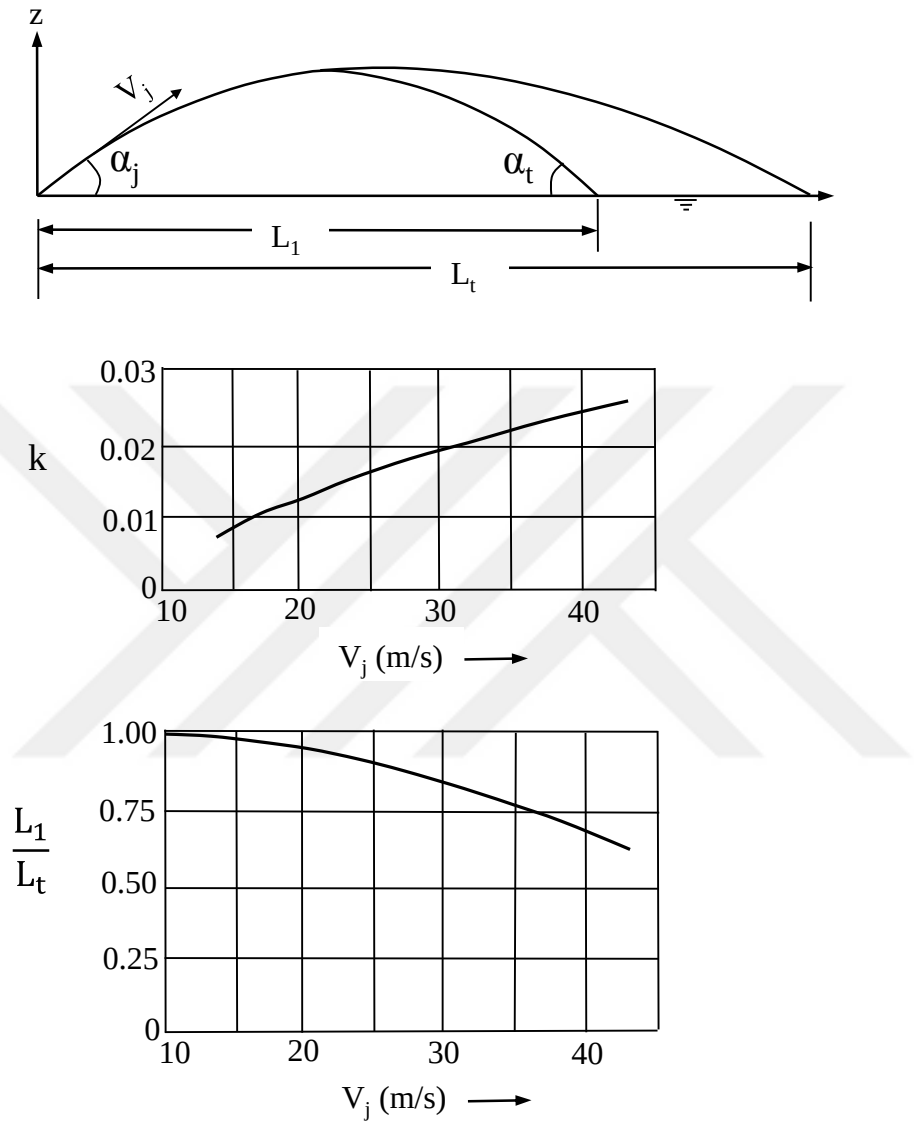

Figure 8 Effect of air resistance on jet trajectory. (Kawakami, 1973)

It is observed that the effect of air resistance is small whenever V_j is less than about 20 m/s but it shrinks the throw distance by about 30% when the velocity is about 40 m/s. However, velocities measured in the model were so low to use the graphs prepared by Kawakami. In order to utilize these graphs prototype velocities must be used. As it was noted before model was constructed by using Froude similarity law. Froude similarity law is;

$(Fr)_m = (Fr)_p$ and $$\frac{V_m}{V_p} = \sqrt{\frac{L_m}{L_p}} = \sqrt{L_r} \quad (7)$$

where $L_r = 1/25$

So prototype velocities can be easily calculated from Eq. (7)

2.3 Head Loss

Main idea of the ski jump is diverting the water jet into the air and creating a jet dispersion. If water jet disperses in the air, large amount of air is entrained into the water jet. This amount of air entrainment reduces the jet velocity and creates significant head losses. Head loss due to the air entrainment can then be calculated by comparing the measured and calculated trajectory lengths. The measured length is affected by the head losses due to air entrainment whereas the calculated length is obtained from the projectile theory without air entrainment therefore no head losses. The difference of the two heads will then be equal to the head loss of the projectile motion of the water jet.

$$H_{j1} = H_{j2} + h_L \quad (8)$$

where

$H_{j1} = \frac{V_j^2}{2g}$ = Jet head without considering air entrainment

$H_{j2} = \frac{V_{j2}^2}{2g}$ = Hypothetical Jet head. (V_{j2} is obtained by using the measured trajectory length L_1 in Eq. (3))

h_L = Head loss due to the air entrainment

CHAPTER 3

EXPERIMENTAL SETUP AND TEST PROCEDURE

3.1 Experimental Setup

The hydraulic model of Laleli Dam and Hydroelectric Power Plant is used as experimental setup of the present study (Figure 9). Hydraulic model is constructed using Froude number similarity law. Length scale of the model is 1:25. The model reservoir is connected to an ogee-crested spillway with a chute angle of $\alpha_s=55^0$. At the end of the chute a circular flip bucket geometry is used into create a ski-jet. The width of the spillway channel is 0.80 m. Vertical drop from lip to riverbed, z_i is 1.2 m. The take-off angle is $\alpha_j=30^0$, bucket radius $R_b=0.60$ m. The geometric elements of the spillway are shown in Figure 10.

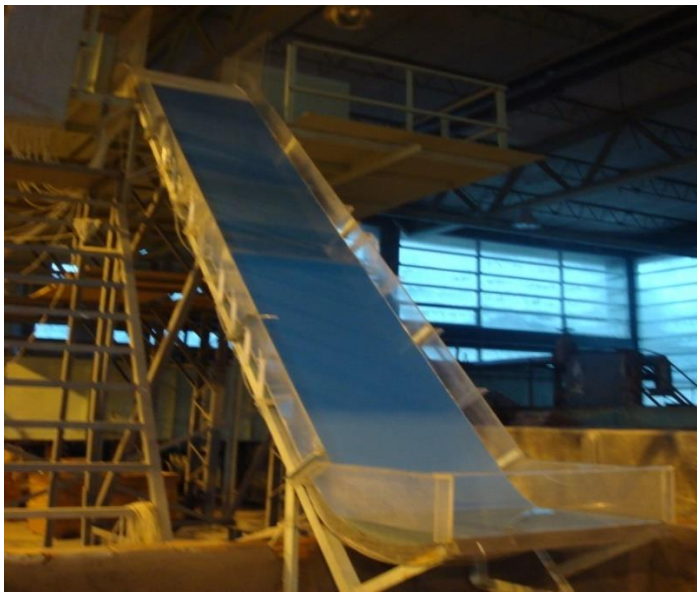

Figure 9 Hydraulic model

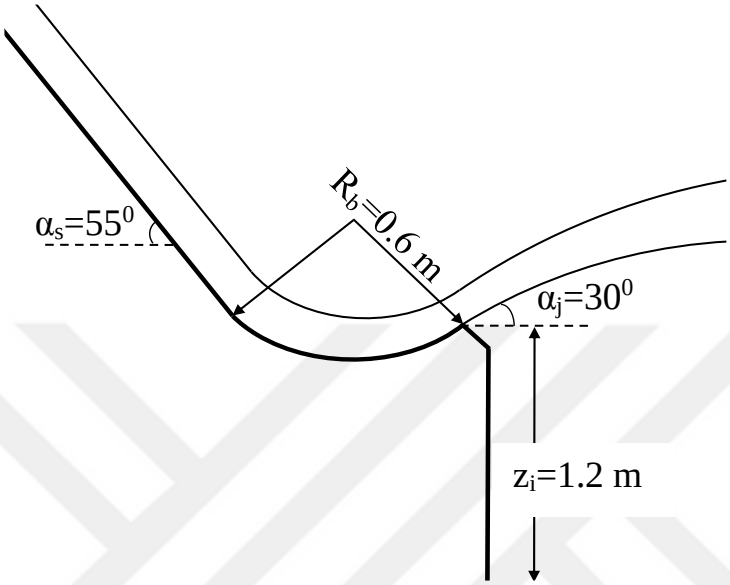

Figure 10 Flip Bucket and related parameters

Huba (Switzerland) pressure transducers are used to record dynamic pressure distribution (Figure 11). 10 transducers were installed in a 2 m long waterproof Plexiglas box and fixed on the ground level at the impact area downstream of the flip bucket (Figure 12).

Figure 11 Huba (Switzerland) Pressure Transducer

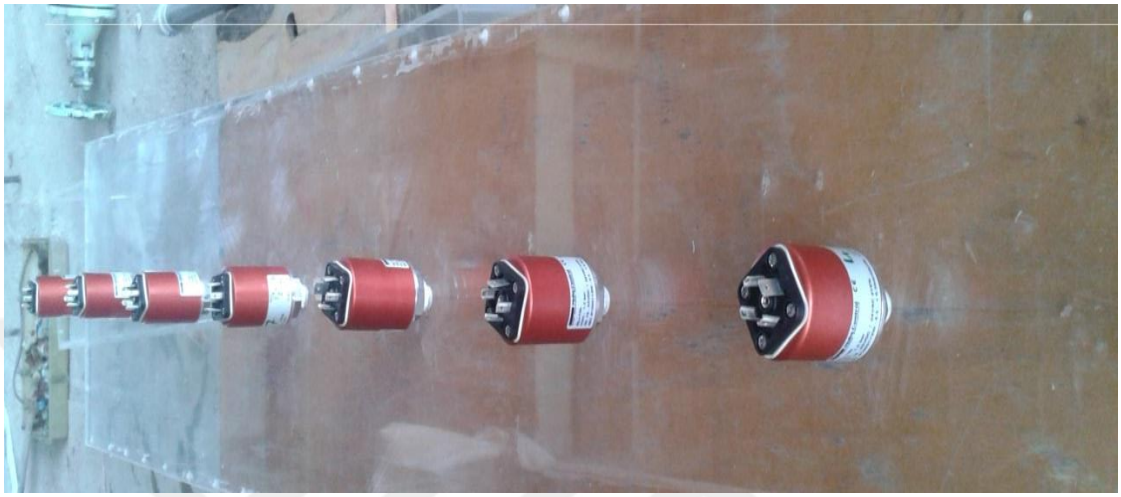

Figure 12 Transducers installed in a Plexiglas box

Measured pressures were recorded in computer memory after digitization. Water level in the downstream of the flip bucket was set by a galvanized plate located at the transition section of the pool to the 1 m wide rectangular measurement channel.

3.2 Experimental Procedure

Water was pumped from the low level reservoir of the laboratory to the elevated tanks and then to the model reservoir. Water was settled in the model reservoir to obtain a constant head before the entrance of the spillway. Discharge was fixed by using valves at the entrance of the model reservoir.

Discharge was adjusted using ogee crest of the spillway. Measurement was done by means of the sharp crested weir at the end of a 1 m wide rectangular measurement channel next to the plunge pool. Before the experiments the water level in the reservoir above the spillway crest was calibrated by the weir. In the experiments the discharge was fixed just by adjusting the reservoir water level.

Once the discharge and the tail water level were established, the flow depth (h_j), velocity head of jet at the bucket lip (H_j), and throw distance to the point of jet impingement $(L_1)_m$ were measured. Velocity at the lip of the flip bucket, V_j, was measured using pitot tube. Dynamic pressures were recorded from each transducer located from the beginning to the end of the jet impact line (Figure 13).

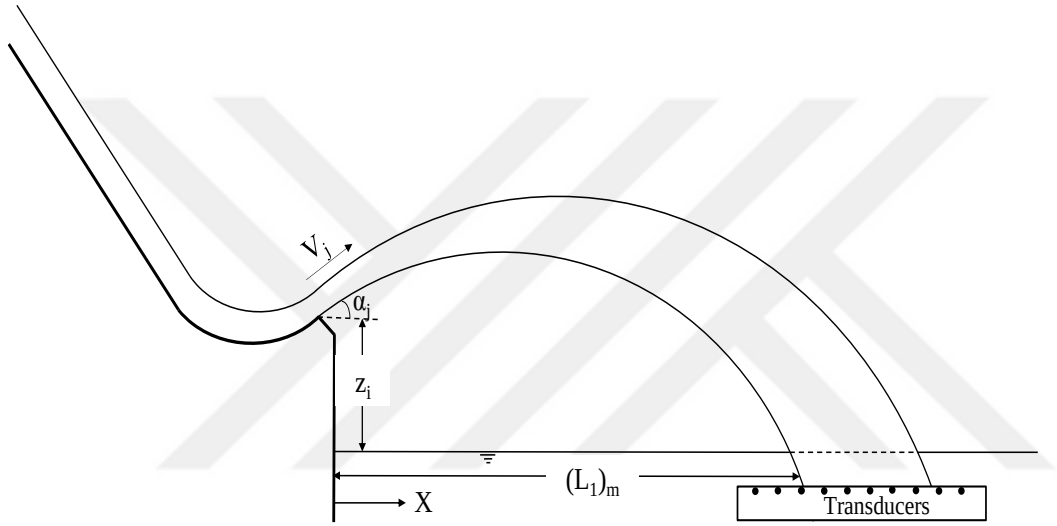

Figure 13 Transducers and measured parameters

10 Huba (Switzerland) pressure transducers were employed to record pressure distribution. Transducers were installed in a 2 m long 0.2x0.1 m rectangular waterproof Plexiglas box. To determine the longitudinal position of the box different water discharges was set before and the impingement distances were measured. After determining the appropriate position of the box for a certain range of experimental discharges, the box housing the pressure transducers was fixed at the bottom of the pool. To test the water resistance and stability of the Plexiglas box some discharges were given without recording the data. There were some problems on the components of the measuring system due to large tractive forces induced by the impinging water jet. After some trials, this kind of structural coupling problems were solved using tougher materials to hold the box stable (Figure 14). Two 1 m wide steel plaques were placed on both sides in lateral direction adjacent to the box to avoid pressure differences owing to the bed level discontinuity. 10

meters long data cables were passed through the plastic pipe covered with a square metal box. These cables were used to record the pressure fluctuations at the bottom of the pool.

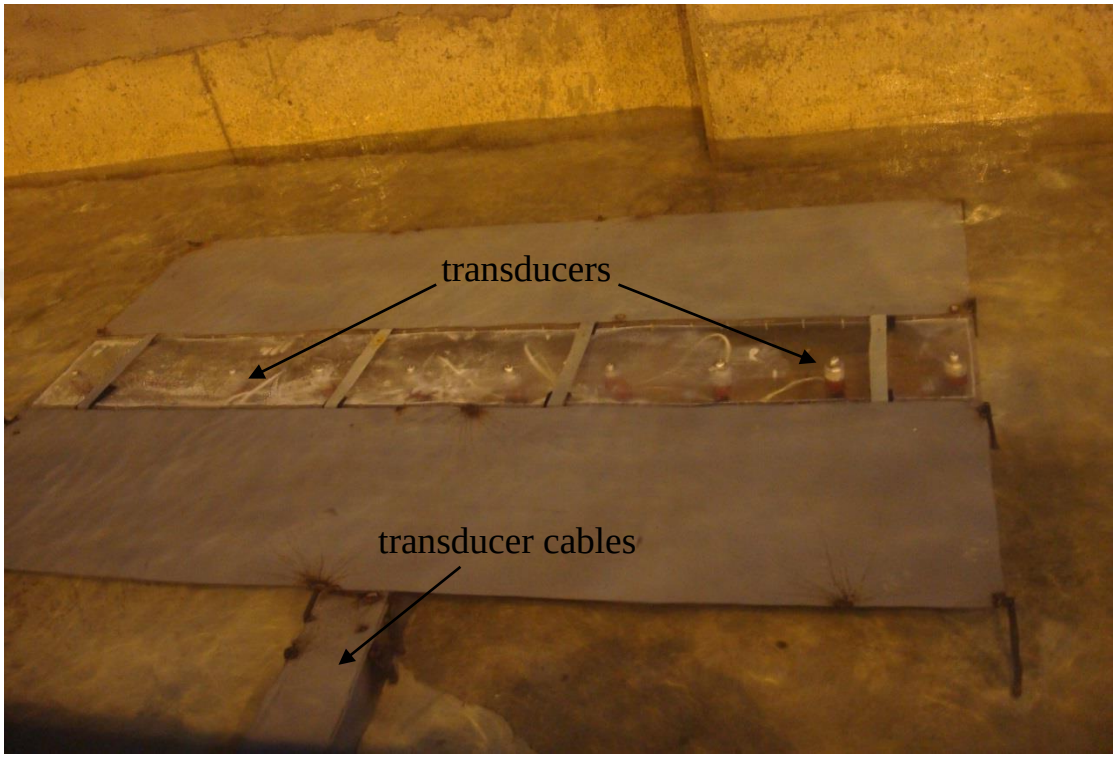

Figure 14 Stabilized Plexiglas waterproof box and side plaques to avoid pressure differences

A computer program named DAQ was run to convert the electronic signals coming from the pressure transducers to digital data. In every single experiment, data were recorded for a period of 180 seconds and digitized at 40 Hz frequency. Experiments were performed for 6 different discharges. Also 6 different tail water depths were tested for each discharge. Totally, 36 different tests were conducted in this experimental study.

To explore the effect of water cushion on the impact of dynamic pressure at the impingement point, tail water level was increased from 0.25 m to 0.75 m with nearly 0.1 m intervals. Tail water level was controlled by a sluice gate placed between the plunge

pool and 1 m wide rectangular channel. Before recording the pressure data a constant tail water level was provided for each test.

3.3 Experimental Results

3.3.1 Discharge Calculation

Head over spillway crest-discharge relationship obtained from preliminary measurements is shown in Figure 15. This relationship was used to adjust the discharge in the experiments.

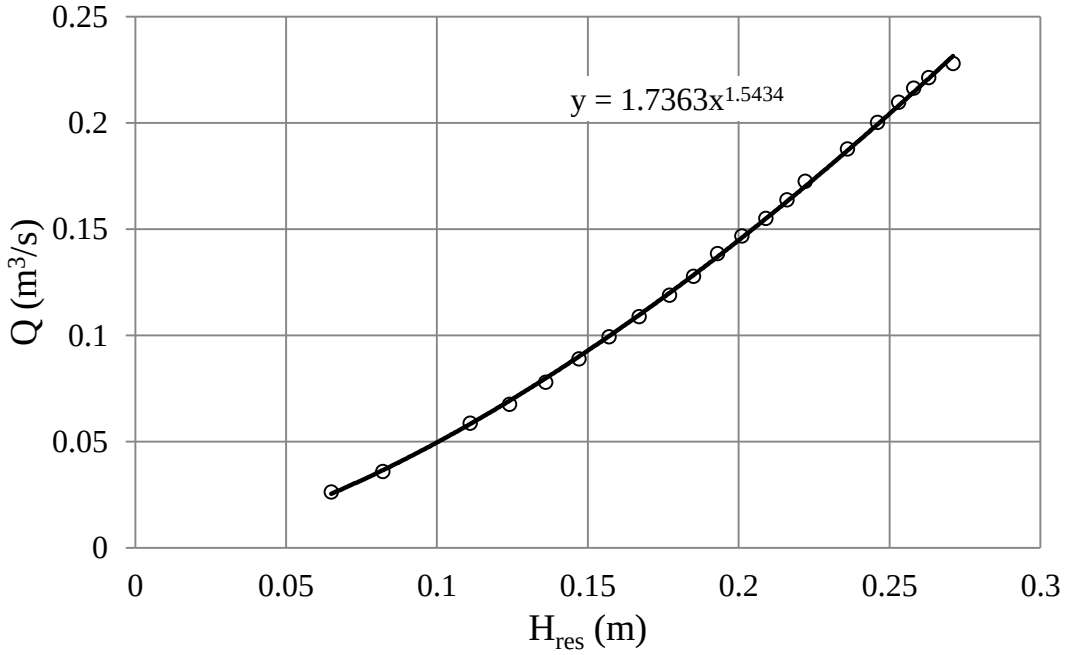

Figure 15 Head over spillway crest- Discharge relationship of the model reservoir

3.3.2 Dynamic Pressure Measurements

The pressure recorded from the transducers represents the total pressure, P_T composed of mean and fluctuating components. The mean pressure in this case is the hydrostatic component, P_H independent of time and the fluctuating component due to large scale

turbulence is named as 'dynamic pressure, P_d'. Subtracting the hydrostatic pressure head from recorded total pressure head, the dynamic pressure head were obtained.

$$\frac{P_d}{\gamma} = \frac{P_T}{\gamma} - \frac{P_H}{\gamma} \quad (9)$$

Where;

P_d/γ = Dynamic pressure head on the ground

P_T/γ = Total pressure head on the ground

P_H/γ = Hydrostatic pressure head on the ground

Dynamic pressure variations at the bed for variable water cushion depths are shown in Figures 16 to 21. Measurements are repeated for the discharges of 0.07, 0.10, 0.13, 0.16, 0.19, and 0.22 m^3/s respectively. Transducers horizontal distances are measured from the bucket lip. One of the transducers (located at X=3.89 m in Figures. 16 and 17, at X=5.29 m in Figures. 18 to 21) malfunctioned therefore its data was removed.

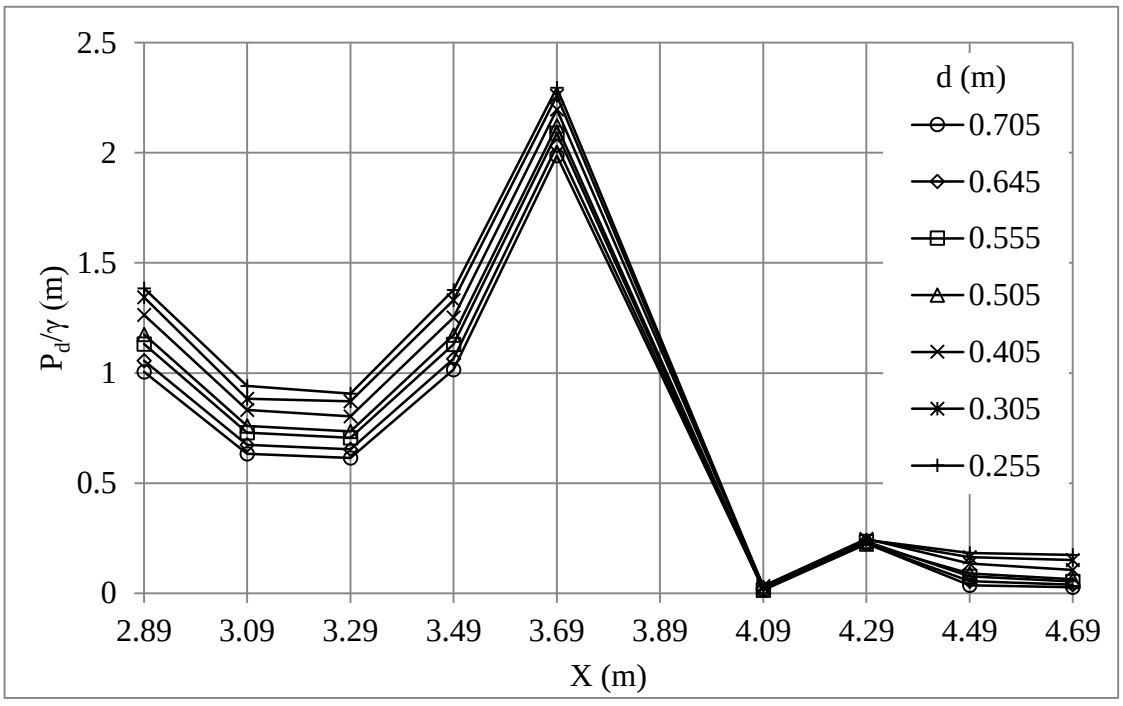

Figure 16 Dynamic pressure variations due to different water depths for Q=0.07 m^3/s

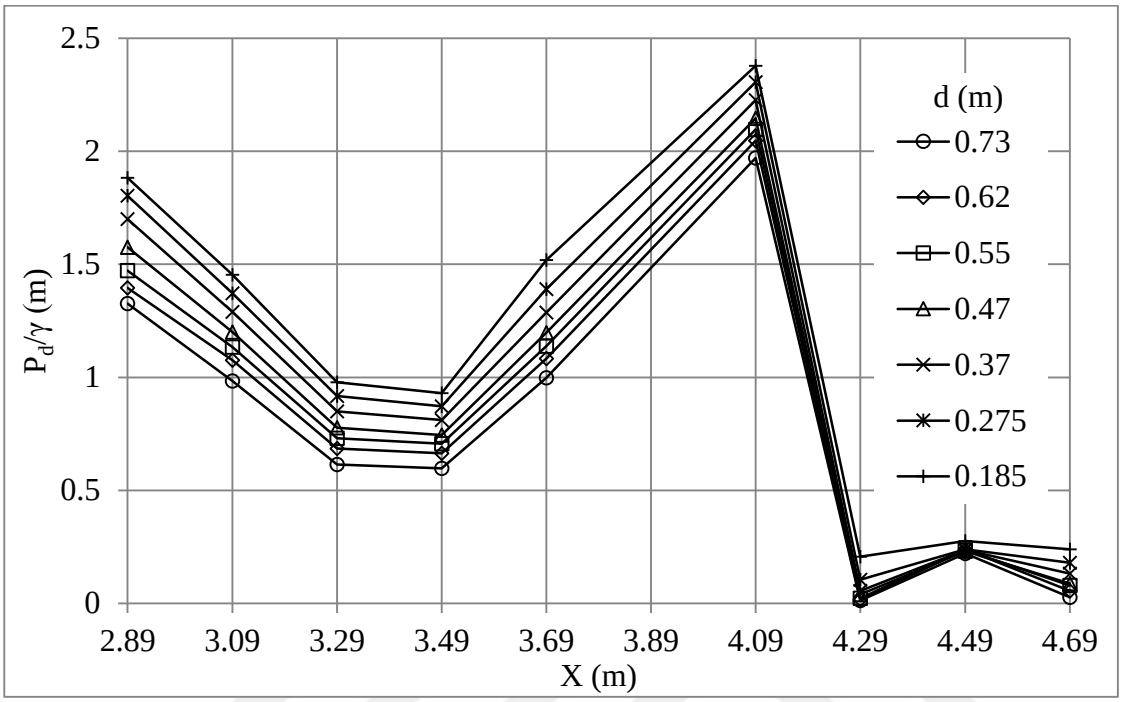

Figure 17 Dynamic pressure variations due to different water depths for Q=0.10 m^3/s

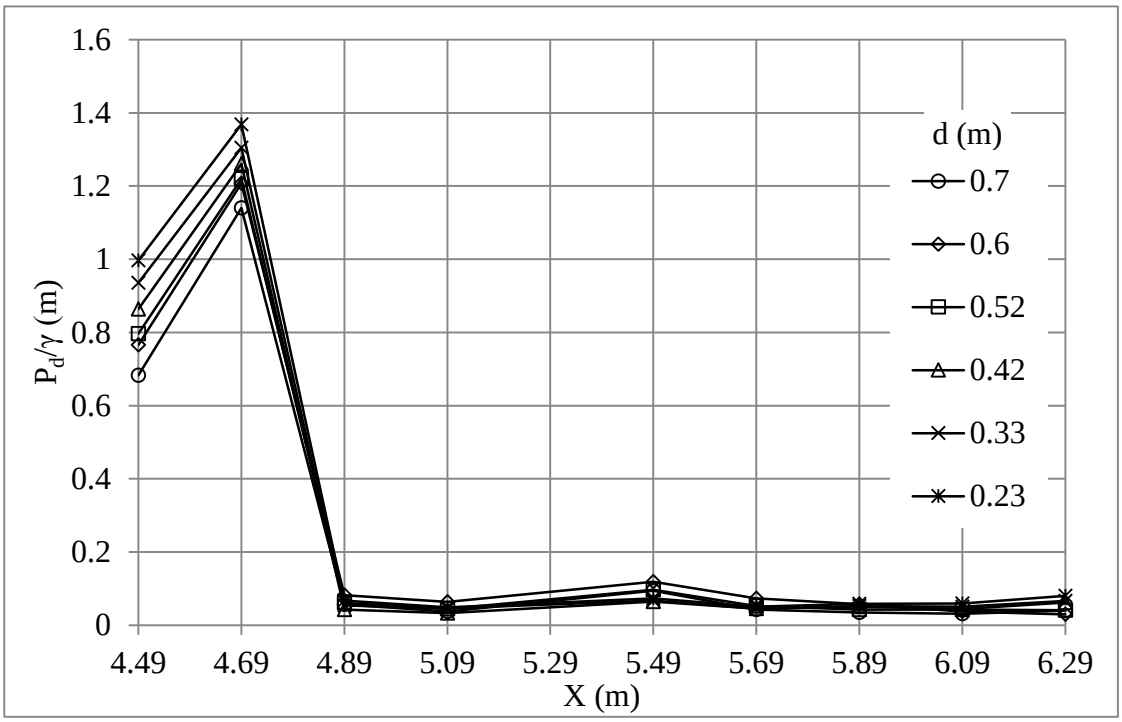

Figure 18 Dynamic pressure variations due to different water depths Q=0.13 m^3/s

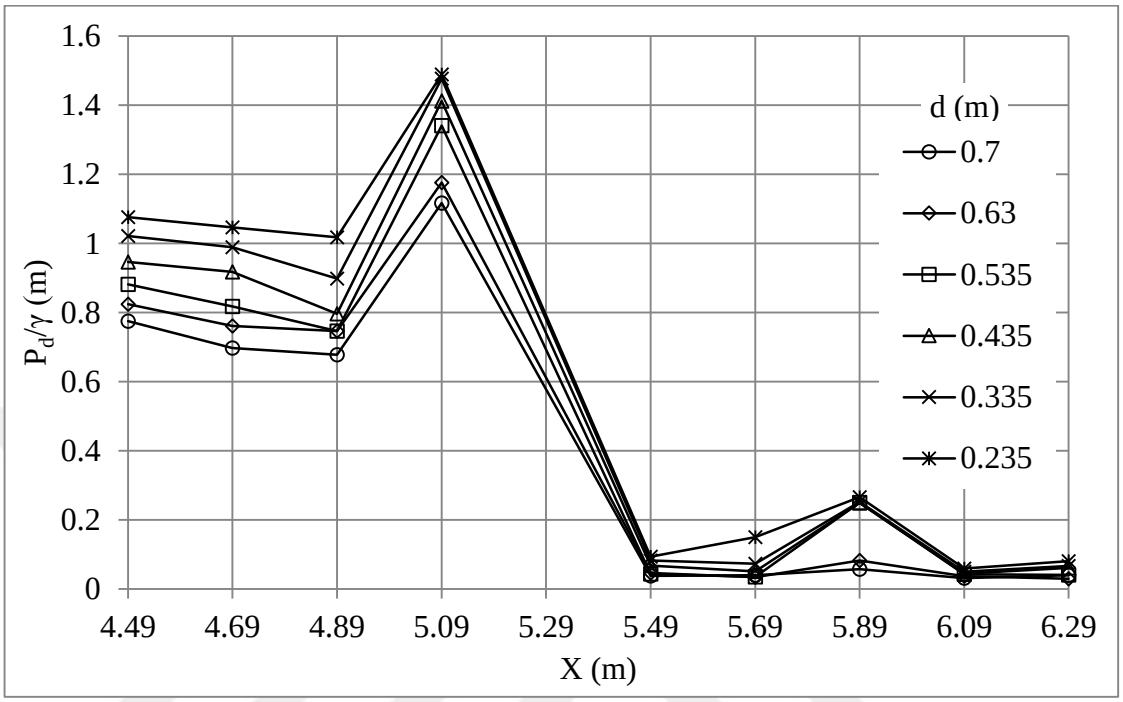

Figure 19 Dynamic pressure variations due to different water depths for Q=0.16 m^3/s

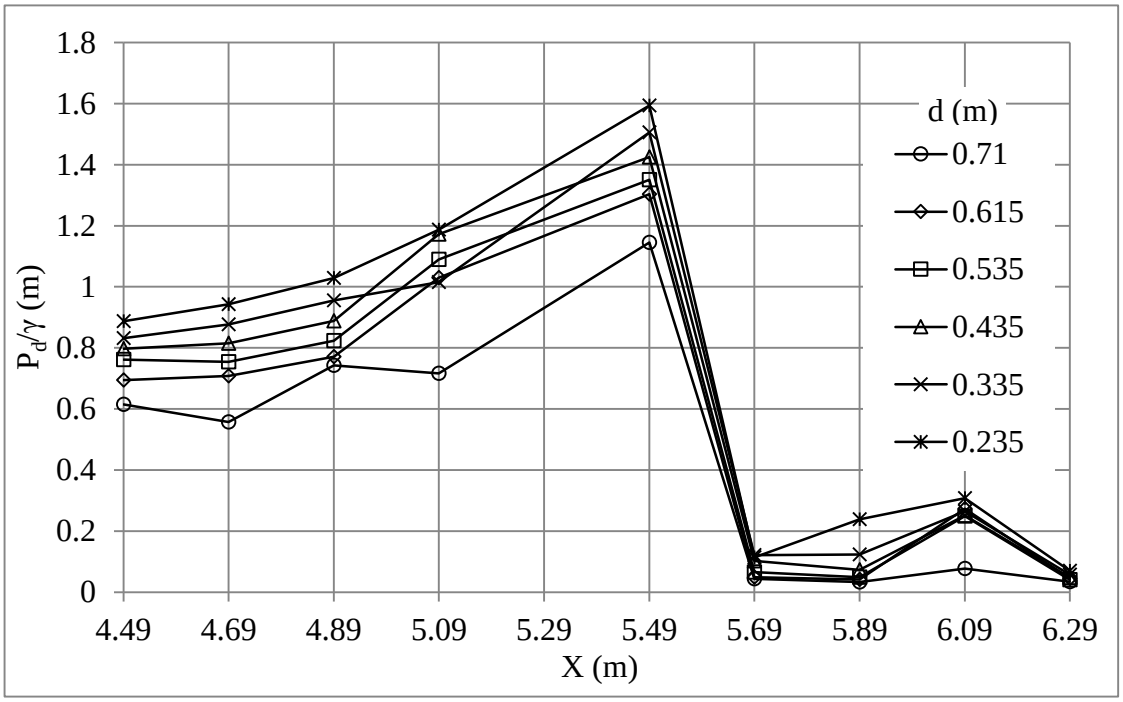

Figure 20 Dynamic pressure variations due to different water depths Q=0.19 m^3/s

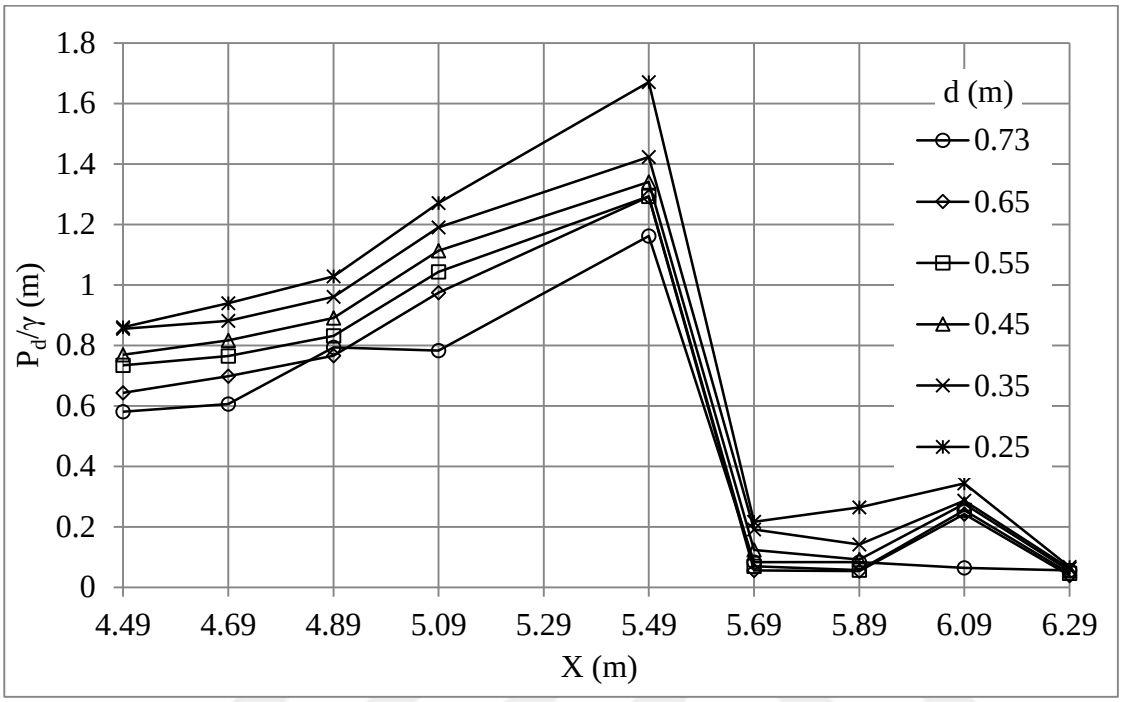

Figure 21 Dynamic pressure variations due to different water depths for Q=0.22 m^3/s

Inspecting the Figures 16 to 21, it can be clearly seen that if the water depth in the plunging area is increased, dynamic pressure impact at the bottom of the riverbed reduces for a constant discharge. However, if the discharge is decreased from 0.220 m^3/s to low discharges gradually, dynamic pressures decrease up to 0.130 m^3/s but then suddenly increases for lower discharges. There is a critical value of discharge somewhere in between 0.130 and 0.100 m^3/s. This increase of dynamic pressure at low discharges is attributed to insufficient aeration of the water jet. Data show that increasing the tail-water depth is not sufficient alone to decrease the impact of the jet on the ground. Also one has to consider large enough discharges to control the impact at the bed by increased aeration rates.

3.3.3 Free Jet Trajectory and Dispersion

Jet head H_j, water depth at the bucket lip h_j, and trajectory length $(L_1)_m$, were measured for all test cases. These measurements are given in Table 1.

Table 1 Measured parameters from the experiments

Q (m^3/s)	H_j (m)	h_j (m)	$(L_1)_m$ (m)
0.22	3.15	0.035	5.49
0.19	2.99	0.031	5.10
0.16	2.75	0.027	5.04
0.13	2.54	0.023	4.67
0.10	2.21	0.019	4.07
0.07	1.73	0.015	3.55

The amount of jet dispersion of water jet in the air was measured from the photos taken during the experiments. Impingement area of the aerated jet was measured to determine the air-water percentage at the point of impact. This area is assumed to be elliptic (Figure 22) and air-water ratios were found based on mass conservation of the water jet. The longitudinal dimension 'b' and the lateral dimension 'a' were determined for each test case and results are summarized in Table 2. Graphical demonstration of the width, a, and length, b, of the jet dispersion can be seen in Figure 23.The photographs indicating the measurement are shown in Figures 24 to 35.

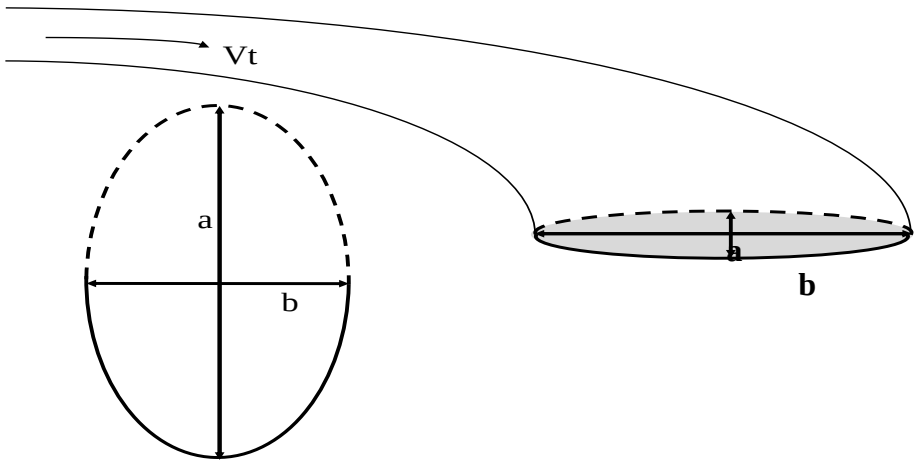

Figure 22 Measurement method of impingement area on the water surface

Table 2 Width, a, and length, b, of the jet dispersed in the air for every single discharge

Q (m^3/s)	a (m)	b (m)
0.22	1.4	1.21
0.19	1.27	0.83
0.16	1.2	0.76
0.13	1.07	0.61
0.10	0.87	0.53
0.07	0.8	0.45

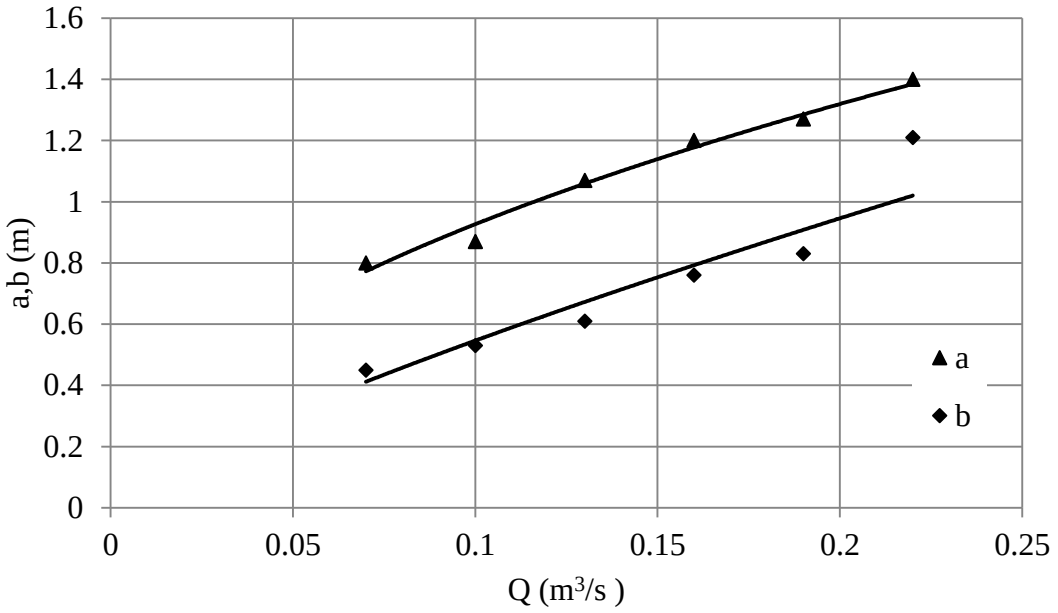

Figure 23 Graphical demonstration of the width, a, and length, b, of the jet dispersion

Figure 24 Width of the dispersed jet for Q = 0.22 m^3/s

Figure 25 Length of the dispersed jet for Q = 0.22 m^3/s

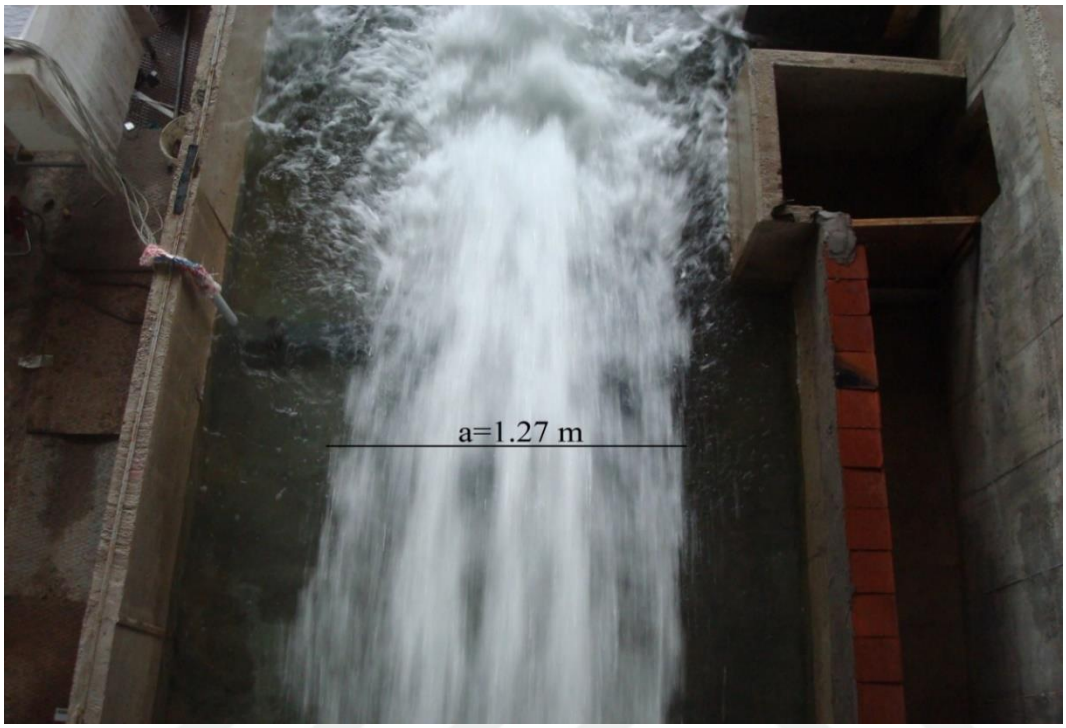

Figure 26 Width of the dispersed jet for Q = 0.19 m^3/s

Figure 27 Length of the dispersed jet for Q = 0.19 m^3/s

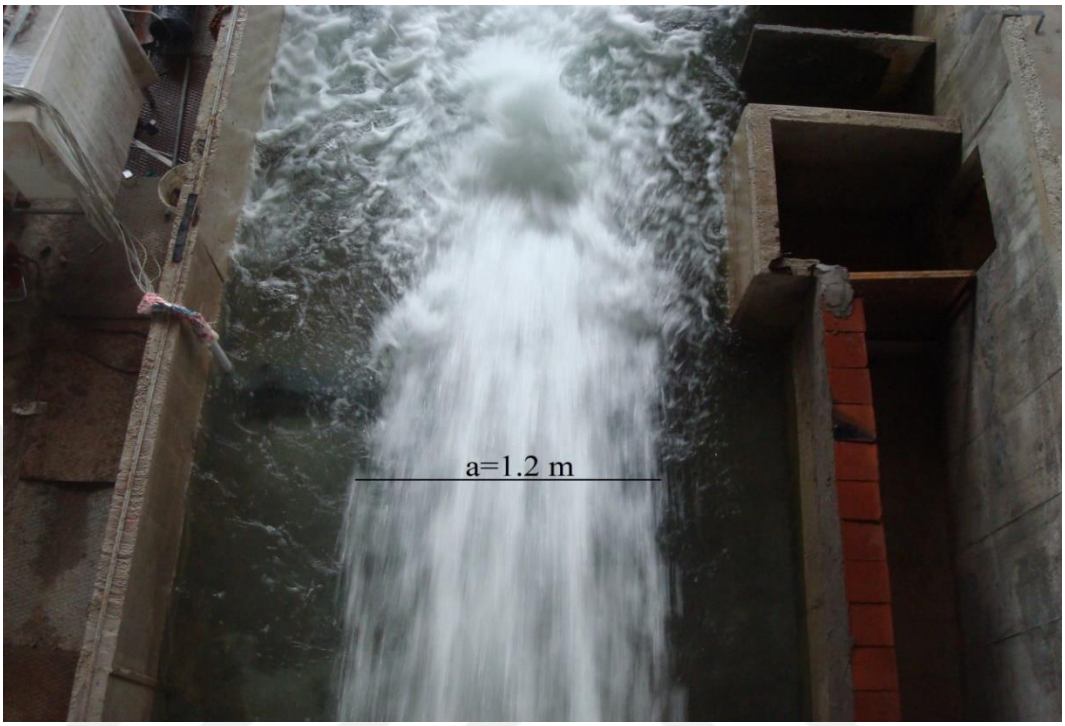

Figure 28 Width of the dispersed jet for Q = 0.16 m^3/s

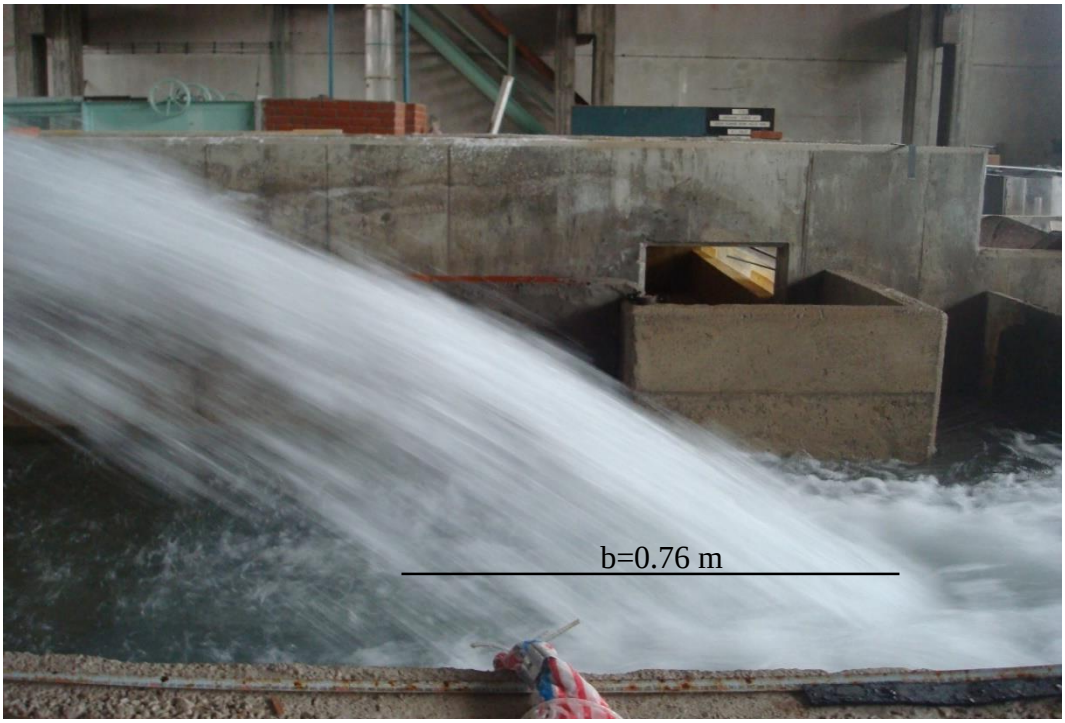

Figure 29 Length of the dispersed jet for Q = 0.16 m^3/s

Figure 30 Width of the dispersed jet for Q = 0.13 m^3/s

Figure 31 Length of the dispersed jet for Q = 0.13 m^3/s

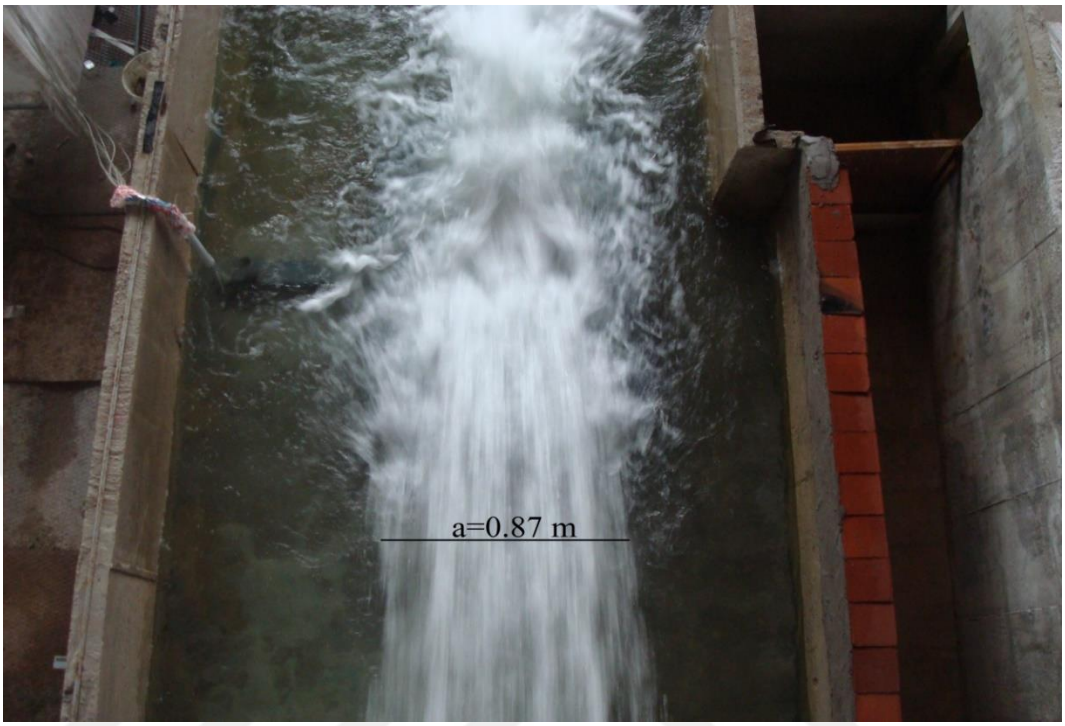

Figure 32 Width of the dispersed jet for Q = 0.1 m^3/s

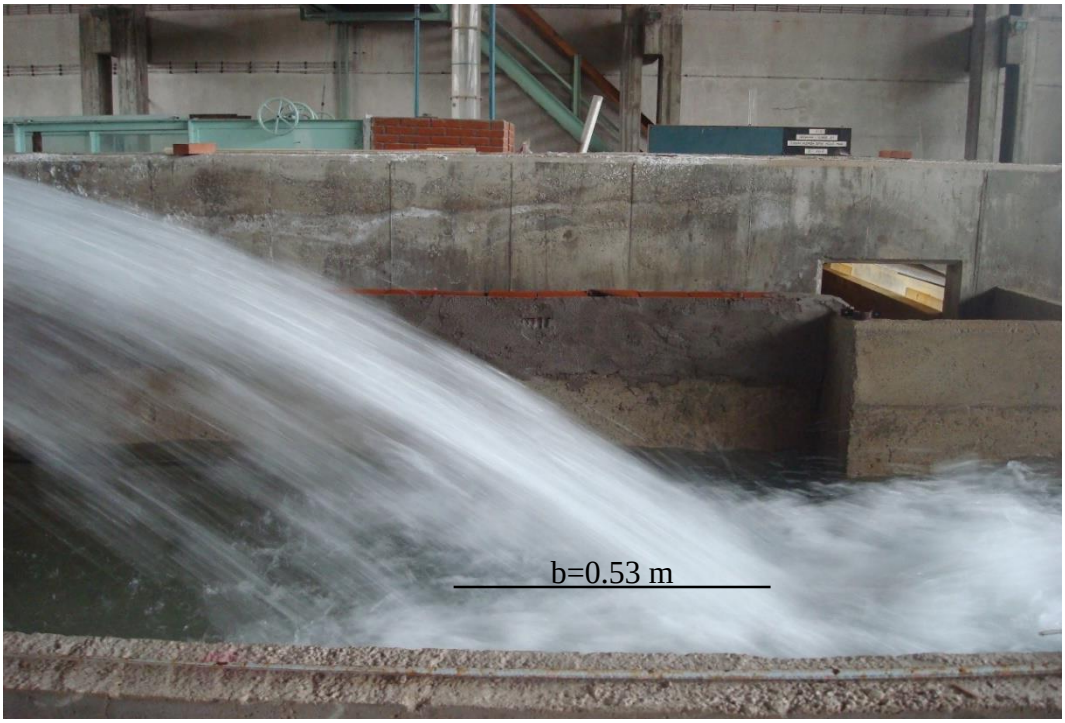

Figure 33 Length of the dispersed jet for Q = 0.1 m^3/s

Figure 34 Width of the dispersed jet for Q = 0.07 m^3/s

Figure 35 Length of the dispersed jet for Q = 0.07 m^3/s

CHAPTER 4

TRAJECTORY FORMULATION AND DISCUSSION OF THE RESULTS

4.1 Introduction

In this chapter, initially, trajectory lengths with and without air entrainment are calculated by empirical formulations. Then, trajectory lengths considering air resistance for every single discharge is compared to measured values. Based on this verification the head loss due to air entrainment, h_L, trajectory velocity, V_t, trajectory angle, α_t are calculated using calculated trajectory lengths considering the effect of air entrainment, $(L_1)_c$. Finally, figures involving dimensionless parameters are given in order to describe the relationship between variables such as trajectory angle and trajectory velocity.

Concerning the impact of the jet, dynamic pressure head distribution was not as influenced asexpected at the beginningof the study from different water depths in the plunging area. For instance, if water depth was increased from 0.25 m to 0.65 m, the reduction of the dynamic pressure was nearly 0.33 m (from 0.93 m to 0.60 m) when water discharge was 0.22 m^3/s. The maximum dynamic pressure head was 1.67 m for the same discharge. However, when the discharge is reduced to 0.07 m^3/s, maximum dynamic pressure head is increased above 2 m for all water depths in the plunging pool. It is obvious that, although water discharge was decreased, dynamic pressure head increased. Therefore, some other parameters in addition to the water depth should be affecting the dynamic pressure head on the riverbed. This will be investigated in the following sections.

4.2 Analysis of Interrelationship between Jet Parameters

4.2.1 Comparison of the Measured and Calculated Trajectory Lengths

As it was mentioned in Chapter 2, the profile of the trajectory leaving a bucket depends on the velocity at the bucket lip and the lip angle. The jet trajectory can be calculated on the basis of projectile theory from Eq. (4). Results of the measured trajectory lengths from the experiments and calculated trajectory lengths from projectile theory are given in Table 3.

Table 3 Comparison of the measured and calculated trajectory lengths

Q (m^3/s)	H_j (m)	$(L_1)_m$ (m)	L_t (m)
0.22	3.15	5.49	7.06
0.19	2.99	5.1	6.77
0.16	2.80	5.04	6.41
0.13	2.54	4.67	5.95
0.10	2.21	4.07	5.32
0.07	1.73	3.55	4.42

On the average, 27 % difference is observed between the measured and calculated trajectory lengths. Trajectory length found by calculation contains no air entrainment or air resistance. But, measured trajectory is reduced by significant amount of air absorbed which turned the water jet into air-water mixture. Hence, its velocity has reduced significantly. Consequently, there is a big difference between the measured and calculated lengths. This retardation due to air mixing, creates a head loss from the jet energy available at the lip of the flip bucket.

4.2.2 Calculated and Measured Trajectory Lengths Considering Air Entrainment

According to the projectile theory, the water jet motion takes place in a frictionless medium. Therefore, velocity does not change throughout the motion. From this point of view, if a measured trajectory length is compared to the one obtained by assuming that the motion occurs in the frictionless environment, the velocity required to pass this length can be easily calculated. Since the environment is frictionless, the lip velocity does not change till the impingement point. Difference between the velocities obtained from the measured and calculated (frictionless) lengths can give the amount of head loss due to the air entrainment.

However, this assumption should be confirmed. Initially, the trajectory length with air entrainment should be computed from Eq. (5). In order to utilize Figure 8 to define the air resistance/air entrainment constant given by Kawakami (1973) prototype velocities are required. Prototype velocities computed from Eq. (7) are given in Table 4.

Table 4 Measured velocities in the model and the corresponding prototype values

Q (m3/s)	Hj (m)	Vj (m/s)	(Vj)p (m/s)
0.22	3.15	7.86	39.29
0.19	2.99	7.66	38.31
0.16	2.80	7.41	37.04
0.13	2.54	7.07	35.33
0.10	2.21	6.58	32.89
0.07	1.73	5.83	29.17

By using the prototype velocity value for each discharge, air resistance constant can be obtained from Figure 8. Then, actual trajectory lengths can be computed from Eq. (5) and compared to the measured length for each discharge. If these values match each other, that means the measurements and the Kawakami formulation confirm to each other, it will be a proof of reliability of the present measurements and validity of the Kawakami formulation. It can also be shown that the difference between the trajectory lengths

calculated with and without air entrainment give the head loss due to air resistance and therefore, prediction of air entrainment rates become possible. Calculation of the trajectory angle (α_t) can also be possible if all components of the energy equation are determined. Comparison of the measured trajectory lengths and calculated trajectory lengths from Eq. (5) can be seen in Table 5.

Table 5 Comparison of the calculated and measured trajectory lengths with air entrainment

$(L_1)_m$ (m)	V_j (m/s)	$(V_j)_p$ (m/s)	k_{from} (Fig. 8)	$(L_1)_c$ (m) (Eq.5)	Error %
5.49	7.86	39.29	0.0250	5.34	2.73
5.4	7.66	38.31	0.0235	5.10	5.55
5.04	7.41	37.04	0.0220	4.78	5.16
4.67	7.07	35.33	0.0210	4.36	6.64
4.07	6.58	32.89	0.0200	3.79	6.88
3.55	5.83	29.17	0.0195	2.98	16.05

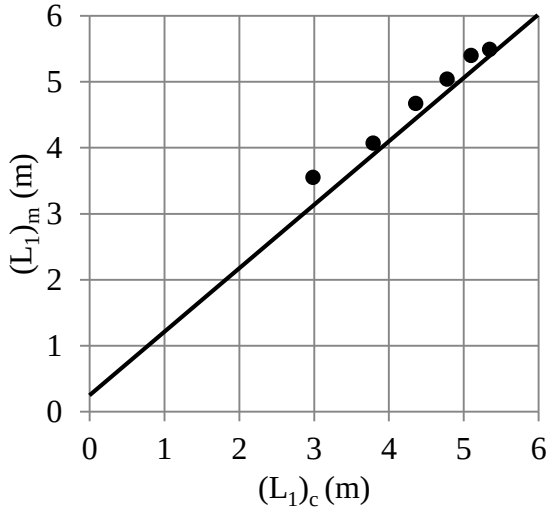

Figure 36 Comparison of the measured and calculated trajectory lengths with air entrainment

Comparison of measured and calculated trajectory lengths are shown in Figure 36. When the arbitrariness in measuring the trajectory length in the model is considered, the agreement is surprisingly good.

4.2.3 Calculation of Head Loss Due to Air Entrainment

Figure 36 shows that measured and calculated trajectory lengths are almost matching up. Average error between the measured and calculated trajectory length is about 7.15 %. Therefore, calculation of head loss due to air entrainment can be reasonable via calculating the velocity difference considering the trajectory lengths by neglecting the air entrainment from Eq. (4). Initially measured jet velocities were used and required trajectory lengths without air entrainment were calculated. Same calculations were made on the lengths by including the air entrainment. Head loss value was calculated using the velocity head difference between calculations from Eq. (8). Head loss calculations are given in Table 6 for the test cases.

Table 6 Head loss due to air entrainment

Q (m^3/s)	V_j (m/s)	V_{j2} (m/s)	H_j (m)	H_{j2} (m)	h_L (m)
0.22	7.86	6.72	3.15	2.30	0.84
0.19	7.66	6.65	2.99	2.25	0.74
0.16	7.41	6.36	2.80	2.06	0.73
0.13	7.07	6.05	2.54	1.87	0.68
0.1	6.58	5.52	2.21	1.55	0.65
0.07	5.83	5.04	1.73	1.29	0.44

4.2.4 Jet Dispersion and Air Entrainment

After jet release from the bucket lip, large amount of air is entrained from the surrounding atmosphere and air-water mixture is formed. To determine the average amount of air entrained from the atmosphere, jet dispersion just before the impingement point was

examined. Since the water discharge and trajectory velocity are known, the water area at the impingement point can be calculated. Air water mixture area was calculated using the dimensions from Figure 24 to Figure 35 given in Chapter 3. Since the water discharge coming from the flip bucket was known, water area was computed at the impingement point easily. If the water area is subtracted from the total area assumed as an elliptic shape, air area at the impingement point can be computed. Relevant calculations and air percentage at the impingement point are given in Table 7. The velocity of water jet at the impingement point, V_t is taken equal to the hypothetical jet velocity, V_{j2}, which was obtained from projectile theory by using measured trajectory length. The water area is obtained by dividing the discharge by V_t. The air area is obtained by subtracting the water area from the measured elliptical area of the mixture at the impingement area. Air percentage is computed from the area percentages of air and water.

Table 7 Aeration ratio of the dispersed jet from the flip bucket

Q (m^3/s)	a (m)	b (m)	A_{total} (m^2)	A_w (m^2)	A_a (m^2)	% air
0.22	1.4	1.21	1.331	0.033	1.298	97.5
0.19	1.27	1	0.998	0.029	0.969	97.1
0.16	1.2	0.76	0.716	0.025	0.691	96.5
0.13	1.07	0.63	0.529	0.021	0.508	95.9
0.1	0.87	0.53	0.362	0.018	0.344	95.0
0.07	0.8	0.45	0.283	0.014	0.269	95.1

Aeration percentages of the impinging jet shown in Table 7 are extremely high. This result directly depends on the height of the bucket lip from tail water, the jet head, and the bucket angle.

4.2.5 Calculation of Trajectory Angle

Trajectory angle, α_t, is also as significant as air entrainment in order to define the dynamic pressure head at impingement point. Now, trajectory angle can be determined by

calculating the horizontal component of the trajectory velocity obtained from Eq. (4). Vertical component of the trajectory velocity head should be equal to the pressure head measured at the impingement point for each discharge value. Energy equation between the bucket lip and impingement point is;

$$H_T = \frac{P_d}{\gamma} + \frac{(V_t \cos \alpha_t)^2}{2g} + h_L$$

where $H_T = z_i + H_j$ (Measured)

h_L = Head loss (calculated)

α_t (to be calculated)

$$\frac{P_d}{\gamma} = \frac{(V_t \sin \alpha_t)^2}{2g} \quad (11)$$

From Eq. (11) trajectory angle, α_t, can be easily calculated. The solution of Eq. (11) for each test case is given in Table 8.

Table 8 Trajectory angle for the test cases

Q (m^3/s)	H_T (m)	$(P_d/\gamma)_m$ (m)	$V_t \sin\alpha_t$ (m/s)	h_L (m)	$V_t \cos\alpha_t$ (m/s)	α_t (^{0})
0.22	4.35	1.67	5.73	0.84	5.99	39.1
0.19	4.19	1.59	5.59	0.74	6.04	42.2
0.16	4.00	1.49	5.41	0.73	5.90	46.2
0.13	3.74	1.42	5.28	0.68	5.68	51.6
0.1	3.41	2.31	6.73	0.65	2.96	59.3
0.07	2.93	2.30	6.71	0.44	1.98	71.5

4.2.6 Evaluation of Measured Dynamic Pressure Data

The maximum dynamic pressure values are shown as function of discharge in Figure 37. If the measured maximum dynamic pressure values inspected carefully, it will be clearly seen that dynamic pressure decreases with decreasing discharge. However, below a critical value, there is a sharp increase in dynamic pressure. This result may be due to

reduced rate of aeration with less air bubbles penetrating the water body in the river. The sudden change in air bubble formation may be due to scale effect in the laboratory where the Reynolds and Weber numbers may be small for small discharges used in the experiments. The ranges of Reynolds and Weber numbers are shown in Figures 38 and 39 respectively. In order to avoid scale effect in aerated flow, the Reynolds number of the jet flow should be above $3x10^5$ and Weber number of the jet flow should be above $2x10^4$ for similar studies (Pfister and Chanson 2012). In Figure 38 Reynolds numbers for the test discharges are below the given limit but they are large enough to establish turbulent flow. Weber number is also an important parameter for this study. According to Figure 39 for the first three test cases with smaller discharges (0.07, 0.1, 0.130 m^3/s) Weber numbers are below the given limit ($2x10^4$). That means aeration mechanisms may be affected in the model study. The measured dynamic pressures for the first two test cases (0.07 and 0.10 m^3/s) are significantly larger indicating that aeration of the water cushion body was not sufficient for those test cases.

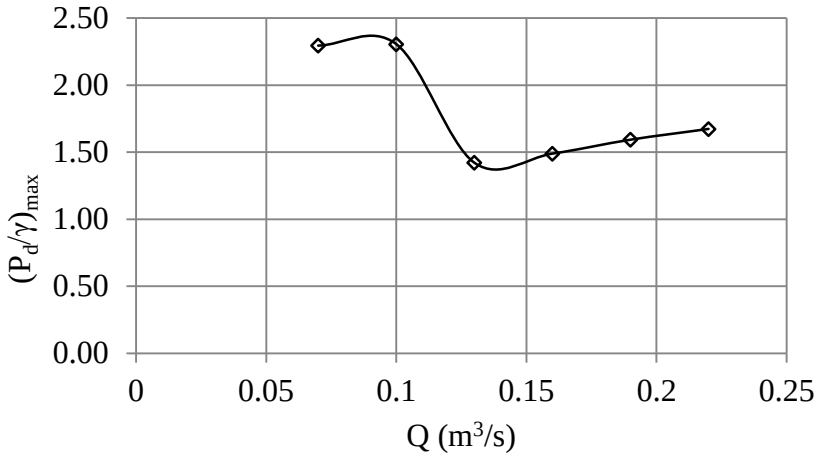

Figure 37 Dynamic pressure variation with respect to water discharge

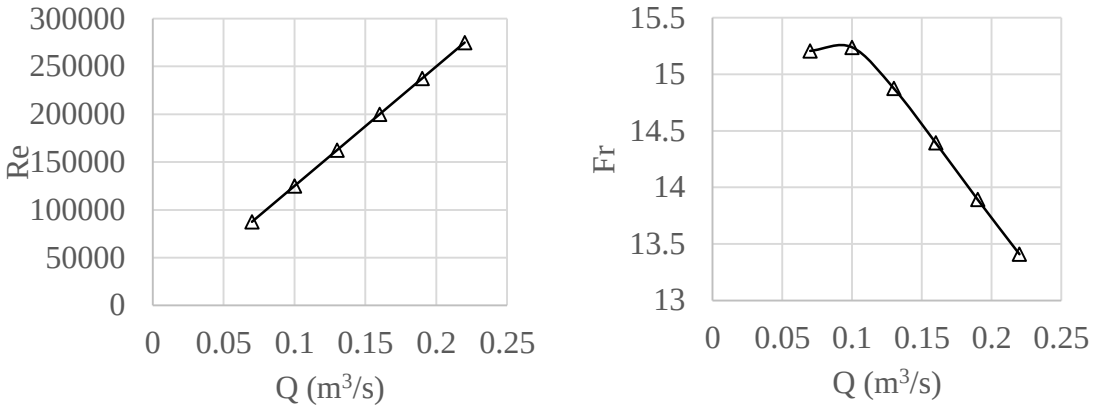

Figure 38 Reynolds number and Froude number as function of discharge

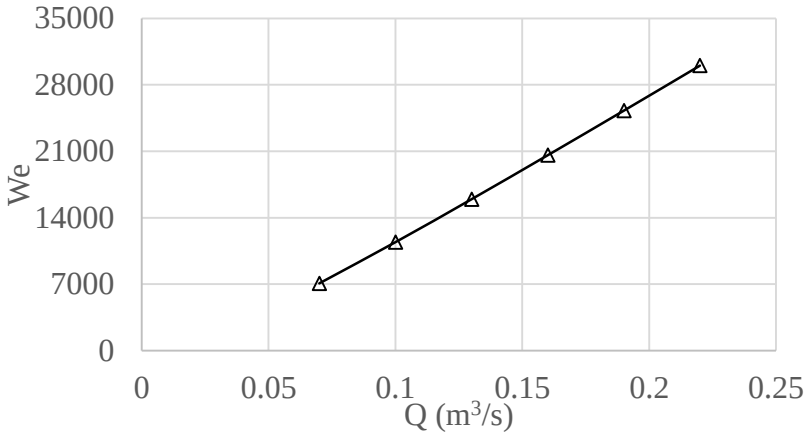

Figure 39 Weber number as function of discharge

The measured dynamic pressure heads are normalized by the total head (P^+) and drawn against the tail water depth, d normalized with the total head (d^+). The results are shown in Figure 40.

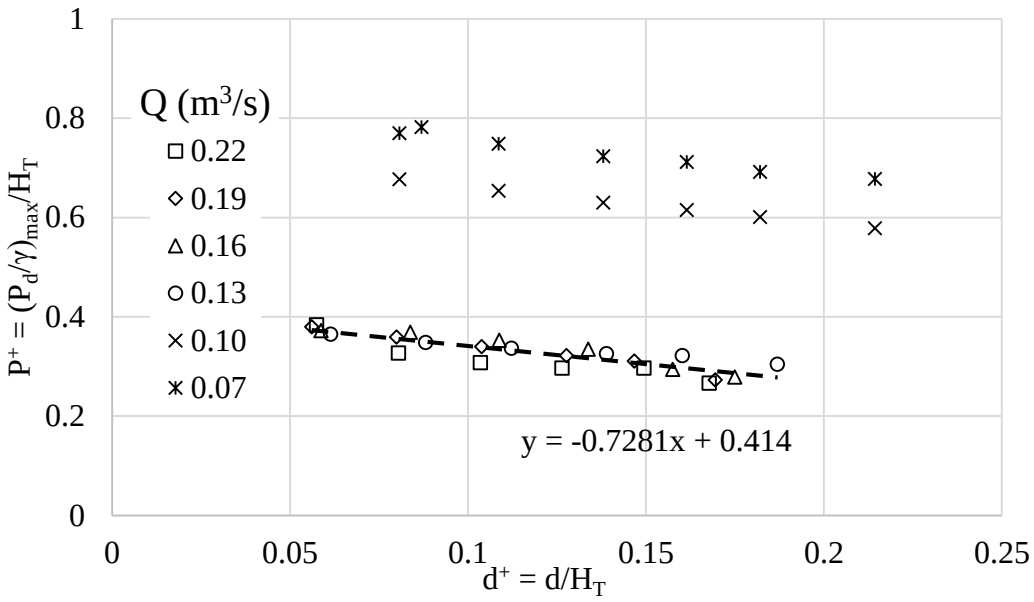

Figure 40 Maximum dynamic pressures to jet head ratio as function of tail water depth to jet head ratio

It is obvious that the measured values of the first two test cases are considerably different than the other four test cases with larger discharges. As discussed above, this may be an indication of insufficient aeration in the model. Therefore, they will not be considered as valid data to discuss the water cushion effect. The measured dynamic pressure head data for discharges 0.130, 0.160, 0.190 and 0.220 m^3/s collapse on to the same line which can be useful to predict the water cushion effect on the dynamic pressures. The best fit line can be written in terms of dimensionless dynamic pressure (P^+) and dimensionless water depth (d^+)

$$P^+ = -0.728(d^+) + 0.414 \qquad (12)$$

4.3 Dimensionless Groups Relevant to Trajectory Angle and Trajectory Length

To simplify the determination of trajectory angle and related parameters, some dimensionless parameters were calculated (Table 9). Determination of the pressure head at the impingement point of the riverbed without conducting any experiments on the model can be possible by using relations between these dimensionless parameters. Dependence between various dimensionless groups is shown in Figures 41-44.

Table 9 Dimensionless Parameters

Q (m^3/s)	α_t	α_t/α_j	H_j/H_T	V_t/V_j	H_j/z_i	$(L_1)_c/H_j$	Fr	Re	We
0.22	39.1	1.3	0.73	0.861	2.7	1.708	13.41	275000	30022
0.19	42.2	1.41	0.72	0.86	2.5	1.71	13.89	237500	25282
0.16	46.2	1.54	0.69	0.859	2.3	1.712	14.39	200000	20584
0.13	51.6	1.72	0.67	0.858	2.1	1.715	14.87	162500	15952
0.1	59.3	1.98	0.64	0.856	1.8	1.719	15.24	125000	11426
0.07	71.5	2.38	0.6	0.854	1.5	1.724	15.21	87500	7092

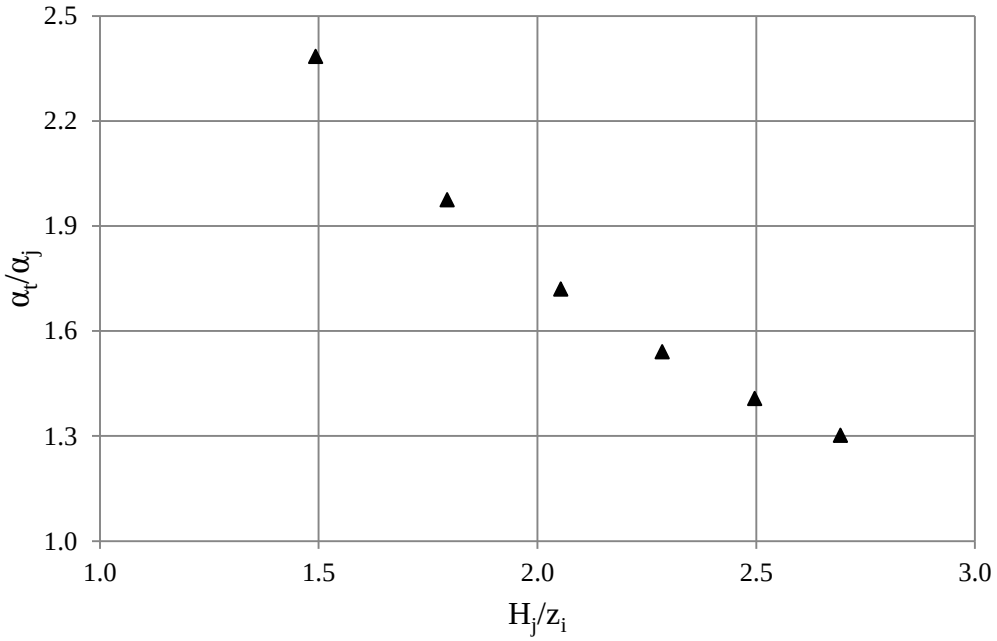

Figure 41 Trajectory angle to jet angle ratio as function of jet head to bucket lip elevation ratio

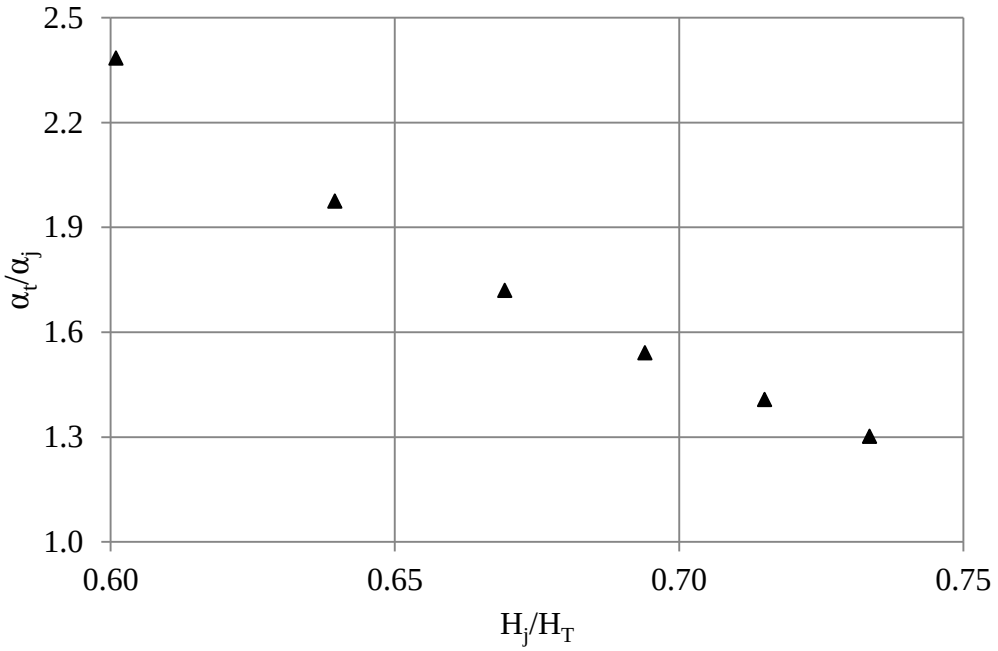

Figure 42 Trajectory angle to jet angle ratio as function of jet head to total head ratio

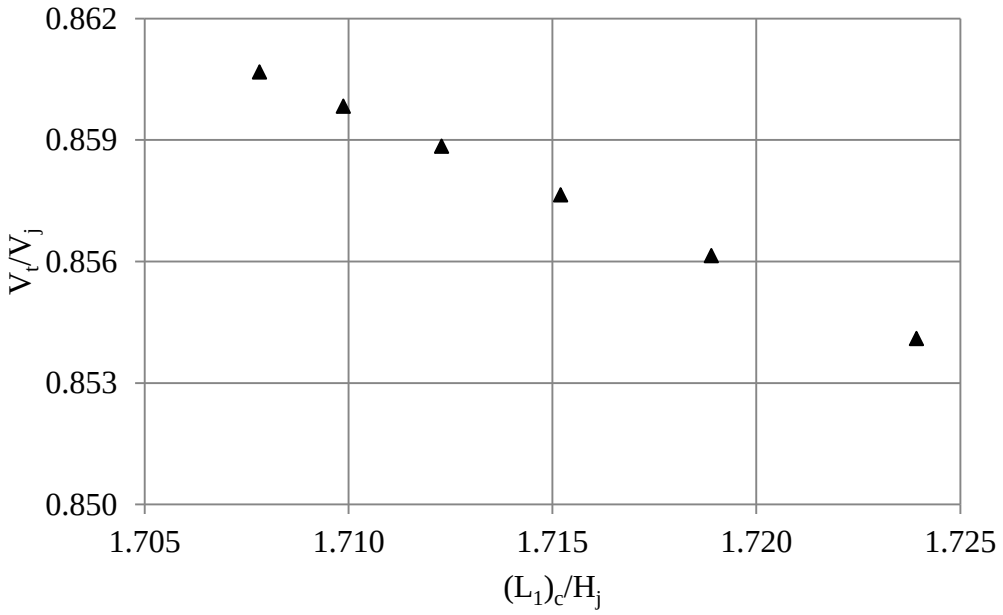

Figure 43 Trajectory velocity to jet velocity ratio as function of throw distance to total head ratio

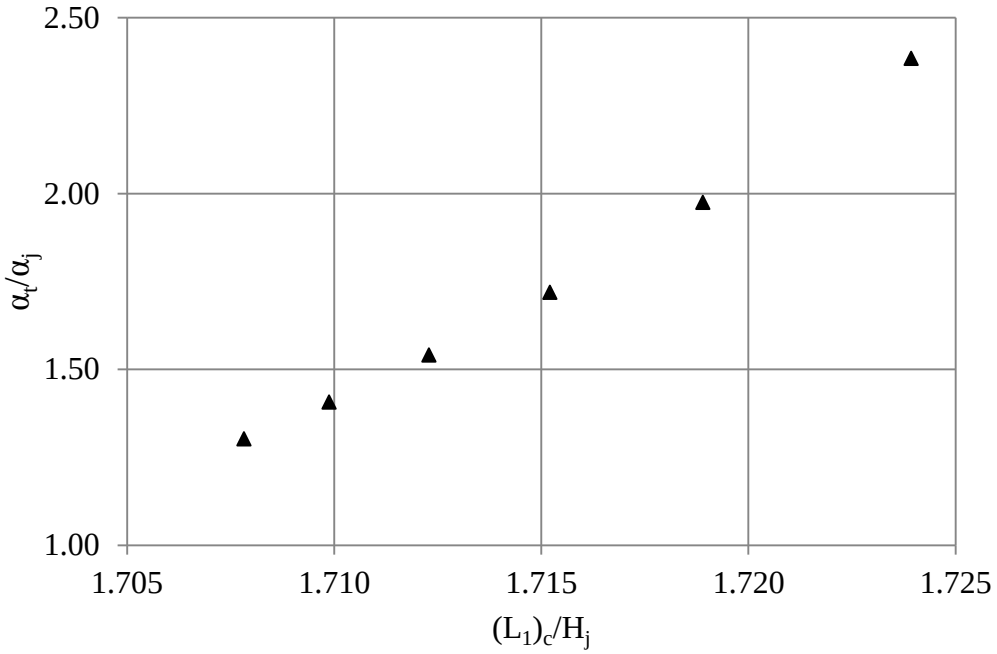

Figure 44 Trajectory angle to bucket angle ratio as function of throw distance to jet head ratio

As observed from Figures 41 to 44 the jet trajectory angle and the jet velocity can be represented as smooth functions of other jet characteristics. Data from all six test cases are included in the graphs. There is no discontinuity observed at low discharges as was observed in dynamic pressures.

The jet trajectory angle increases significantly with decreasing discharge (Figures 41 and 42, Table 8). Large trajectory angle means the jet is almost normal to the bed at the impingement point. Therefore, larger dynamic pressures are developed on the bed at low jet discharges. This may be another reason for increasing dynamic pressures at low discharges.

CHAPTER 5

CONCLUSIONS

In the present study impact of water jet from a flip bucket on the impingement point on the river bed has been studied. Effects of aeration and water depth at the impingement point on the dynamic pressures were investigated experimentally. Empirical equations were used to calculate the jet trajectory length and impact angles. The computed trajectory lengths were compared to measured ones for the six different test discharges. From this experimental study, the following conclusions can be drawn:

i. Dynamic pressure is not directly proportional to the water discharge coming from the flip bucket. The trajectory angle and the amount of air entrainment must be considered.

ii. Air entrainment affects the trajectory length and trajectory angle which are more effective in energy dissipation than the tail water depth.

iii. An expression (Eq.12) for predicting the dynamic pressures on the impingement point has been developed as a function of dimensionless tail water depth.

iv. A significant increase in dynamic pressures were observed for jet discharges less than 0.130 m^3/s for which Weber number goes below $2x10^4$. This behavior was partly attributed to less air bubble penetration into the water cushion, a result of scale effect specific to the present experimental set-up. This situation would not

occur in real structures since the Weber numbers are expected to be larger than the limiting value.

v. For decreasing discharges the trajectory angle increases which also increases the jet impact at the impingement point and therefore dynamic pressures. The maximum discharge may not produce the maximum dynamic pressures. Therefore, discharges smaller than the maximum should also be considered in the analysis and design stages of the flip bucket type energy dissipators.

vi. Dimensionless plots for the jet velocity and trajectory angles are prepared that can be used to study impact conditions at the impingement points for various discharges. However, these plots are valid for a bucket angle of 30 degrees.

REFERENCES

Ervine, D. A. The entrainment of air in Water -Water Power and Dam Construction, 1976, 28(12).

Hartung, F.; Hausler, E. Scour, stilling basins and downstream protection under overfall, 11th ICOLD. Madrid, 1973.

Juon, R.; Hager, W. H. Flip bucket without and with deflectors, Jrnl. of Hyd. Eng. ASCE, November 2000.

Kawakami, K. A study on the computation of horizontal distance of jet issued from a ski-jump spillway; Trans Japan Society of Civil Engineers. 1973; Vol. 5.

Khatsuria, R. M. "Hydraulics of Spillways and Energy Dissipators" 2005

Laleli Dam and HEPP Spillway Hydraulic Model Studies, Hydromechanics Laboratory, Civil Engineering Department, METU, March 2012.

Lenau, C. W.; Cassidy, J. J. Flow through spillway flip buckets. ASCE Jrnl. of Hyd. Dn. May 1969.

Mason, P. J. The choice of hydraulic energy dissipator for dam outlet works based on a survey of prototype usage. Proc. Instn. Civil Engineers, Part I. May 1982, 72.

Mason, P. J. Erosion of plunge pools downstream of dams due to the action of free trajectory jets. Proc. Inst. Civil Engineers. Part I. May 1984.

Mason, P. J.; Arumugam, K. Free jet scour below dams and flip buckets. Proc. ASCE, Hyd. Dn. February 1985.

Mason, P. J. Effect of air entrainment on plunge pool scour. ASCE Jrnl. of Hyd. Eng. March 1989.

Mason, P. J. Practical guide lines for the design of flip buckets and plunge pools, Water Power and Dam Construction, Sept. /Oct. 1993.

Mriouah, D. ‘‘Crues Importantes imprevues: cas du barrage de Oued el Makhazine all Maroc’’, Q-63, R-82 Proc. 16th ICOLD. San Francisco, June 1988.

Moric, P. ‘‘Questioning the need for spillways’’, International Water Power & Dam Construction, January, 1997.

Peterka, A. J. Hydraulic design of stilling basins and energy dissipators, USBR, Eng. Monograph, No.25, 1978.

Rudavsky, A. B. Selection of spillways and energy dissipators in preliminary planning of dam developments, 12th ICOLD, Q 46, R 9 Mexico, 1976.

Schmocker, L.; Pfister, M.; Hager, W.H.; Minor, H.E. Aeration characteristics of ski jump jets. ASCE Jrnl. Of Hyd. Dn. 2008.

‘‘Seminar on Safety Evaluation of Existing Dam for Foreign Engineers – History of Dam Safety Development in the U.S.’’ USBR, 1983.

Takasu, S.; Yamaguchi, J. ‘‘Principle for selecting type of spillway for flood control dams in Japan’’, Q-63, R-19, ibid, 1988.

Tsung, S.C,; Lai, J.S,; Young, D.L. Velocity Distribution and discharge calculation at a sharp-crested weir, Paddy Water Env. 12:203-212, June 2013.

Vischer, D.; Rutschmann, P. ‘‘Spillway facilities – Typology and General Safety Questions’’, Q-63, R-23, Proc. 16th ICOLD. San Francisco, June, 1988

Pfister M. And Chanson H. (2012) ‘Discussion: Scale effects in physical hydraulic engineering models’, Journal of Hydraulic Research, 50(2):244-246

Pfister M.and Hager W. (2010b) ‘Chute aerators II: Hydraulic Design’, Journal of Hydraulic Engineering, 136(6): 360-367

USBR (1987) ‘Design of Small Dams’, United States Department of the Interior Bureau of Reclamation, Page:339